Age-dependent glycomic response to the 2009 pandemic H1N1 influenza virus and its association with disease severity

Shuhui Chen, Brian Kasper, Bin Zhang, Lauren P. Lashua, Ted M. Ross, Elodie Ghedin and Lara K. Mahal*

KEYWORDS: H1N1, influenza, host response, lectin microarray, glycomics, high mannose

ABSTRACT

Influenza A viruses cause a spectrum of responses, from mild cold-like symptoms to severe respiratory illness and death. Viral strains and intrinsic host factors, such as age, can influence the severity of the disease. Glycosylation plays a critical role in influenza pathogenesis, however the molecular drivers of influenza outcomes remain unknown. In this work, we characterized the glycomic response to the H1N1 2009 pandemic influenza A virus in age-dependent severity. Using a ferret model and a lectin microarray technology we have developed, we compared responses in newly weaned and aged animals, a model for young children and the elderly, respectively. Glycomic analysis revealed changes in glycosylation over the course of the infection, that were associated with severity in an age-dependent manner. These responses may help explain the differential susceptibility to influenza A virus infection of young children and the elderly.

1

INTRODUCTION

Influenza A viruses cause a spectrum of responses from mild cold-like symptoms to severe respiratory illness and death.[1] Both viral strains and intrinsic host factors, such as age, influence disease severity.[2] In general, infants, young children and individuals older than 65 are more likely to have severe clinical outcomes upon influenza infection. However, during pandemic outbreaks, influenza viral strains can emerge that shift the age-dependent infection patterns. In 2009, a novel H1N1 influenza strain (H1N1pdm09) emerged that caused severe clinical symptoms more frequently in older children and adults than in young children and the elderly.[3] The lack of response in the elderly was attributed to pre-immunity due to prior waves of seasonal and pandemic influenza strains generating neutralizing antibodies.[4-7]

The ferret model of influenza mimics clinical outcomes for the H1N1pdm09 across the age spectrum.[8-10] Ferrets are an attractive animal model for influenza as they share similar lung physiology to humans and recapitulate the pathology observed in clinical populations. In addition, human influenza viruses efficiently replicate in ferrets without the need for adaptation, enabling study of the original viral strains.[11] This is due to the fact that ferrets contain the receptor for human influenza, α-2,6-sialic acids, in their upper respiratory tracts. The similarities between the glycans in the respiratory tract of ferrets to those observed in humans also make this a good model to study glycomic changes in response to influenza infection.[12, 13]

Glycosylation plays an important role in influenza infection and host response.[14, 15] Adhesion of viral hemagglutinin (HA) to host receptors containing terminal α-2,6-sialic acids located in the upper respiratory tract is the first step in the infection process. Release of viral particles requires viral neuraminidases (NA) to cleave sialic acids.[16] This enzyme is the target of current therapeutics against influenza.[17, 18] Due to the importance of HA, NA and sialic acid in influenza biology, the

2

majority of glycomic analysis has focused on these molecules. In previous work, our laboratory used lectin microarray technology to systematically examine the glycomic response to H1N1pdm09 in an adult ferret population.[19] We found that severity was not related to sialic acid levels, but rather was correlated with the expression of high mannose. This glycan motif is the recognition element for a host of innate lectins that activate the immune system. The complement inducing lectin MBL2, which binds this induced glycan epitope has been strongly associated with influenza severity.[20, 21] We hypothesize that the induced high mannose may play a causative role in the damage observed from MBL2 levels in influenza.

In this work, we profile glycomic changes, including high mannose, over the course of infection with the pandemic 2009 H1N1 strain of influenza and determine whether they overlay differences in severity observed with age in the ferret model. Since their introduction in 2005,[22] lectin microarrays have been used to perform glycomic analysis on a wide variety of samples from microvesicles[23] to human tissues.[24] Herein, we analyze the glycomic response to H1N1pdm09 infection in newly weaned and aged ferrets using our dual-color lectin microarray technology.[25] We also compare the baseline glycomes of newly weaned, adult, and aged ferrets. Our data suggest that differences in the glycome, in particular in the high mannose response, may help explain the variation in clinical outcomes as a result of influenza infection.

METHODS

Infection of ferrets with H1N1pdm09

Fitch ferrets (*Mustela putorius furo*, female) were obtained from Triple F Farms (Sayre, PA) and verified as negative for antibodies to circulating influenza A (H1N1 and H3N2) and B viruses. Newly weaned ferrets were defined as 6-7 weeks of age, adult ferrets as 6-12 months of age, and

3

aged ferrets as 5.5-7 years of age. Ferrets were pair-housed in stainless steel cages (Shor-Line, KS) containing Sani-Chips laboratory animal bedding (P.J. Murphy Forest Products, NJ) and provided with food and fresh water *ad libitum*. Newly weaned and adult ferrets were administered intranasally the H1N1pdm09 virus, A/California/07/2009 (Influenza Reagents Resources (IRR), BEI Resources, the Centers for Disease Control and Prevention, VA) at a dose of 10^6 PFU. Aged ferrets were infected at a dose of 10^5 PFU. The animals were monitored daily for weight loss and disease symptoms, including elevated temperature, low activity level, sneezing, and nasal discharge. Animals were randomly assigned to be sacrificed at day 1, 3, 5, 8, or 14 post-infection (DPI) or euthanized if their clinical condition (e.g., loss of >20% body weight) required it.

Tissue Collection

Necropsies were performed to collect lung tissue. Lungs were rinsed with cold PBS and the right upper and lower lung lobes were removed. Each lobe was sectioned into quadrants and snap frozen prior to preparation for lectin microarray analysis.

Definition of Severity Metrics

Severity of infection was determined for all animals studied who were sacrificed at day 8 post-infection. We analyzed two different metrics: weight loss and pneumonia composite score (PCS). In both cases, we determined the cutoffs for mild, moderate and severe by quartile wherein mild = Q0-Q1, moderate = Q1-Q3, severe = Q3-Q4. Weight loss cutoffs for adult ferrets: mild (weight loss <10.8%), moderate (weight loss: 10.8%-16.5%) and severe (weight loss >16.5%). Cutoffs for aged ferrets: mild (weight loss <18.3%), moderate (weight loss: 18.3%-21.9%) and severe (weight

4

loss > 21.9%). PCS cutoffs newly weaned ferrets: mild (PCS < 8.5), moderate (PCS: 8.5-10.5) and severe (PCS > 10.5). For adult ferrets: mild (PCS <8), moderate (PCS: 8-10) and severe (PCS > 10). For aged ferrets: mild(PCS < 8.5), moderate (PCS: 8.5-11), and severe (PCS > 11).

Lectin microarray

Ferret lung tissue samples were washed with PBS supplemented with protease inhibitors cocktails (PIC) and sonicated on ice in PBS with PIC until completely homogenous. The homogenized samples were then labeled with Alexa Fluor 555-NHS as previously described.[26] Reference sample was prepared by mixing equal amounts (by total protein) of all samples and labeling with Alexa Fluor 647-NHS (Thermo Fisher). **Supplementary Table 1** summarizes the print list for each experiment. Printing, hybridization and data analysis were performed as previously described.[27]

Data Availability

Data is available at DOI: 10.7303/syn22176606.

RESULTS AND DISCUSSIONS

Ferret lung glycosylation alters with age.

Clinical outcomes and susceptibility to influenza infection vary with age.[28,29] Given the role host glycans play in influenza infection and immune response, we characterized the baseline glycosylation in the lungs of uninfected female ferrets from three age categories: newly weaned,

adult and aged. Newly weaned ferrets were defined as those from 6-7 weeks of age. The course of H1N1pdm09 infection in this ferret population mirrors that observed clinically in young children, i.e. a mild to moderate presentation of symptoms.[9] Adult ferrets, defined as 6-12 months of age, have more varied responses to H1N1pdm09 infection ranging from mild to severe, again in line with human populations.[8] Aged ferrets, defined as 5.5-7 years of age, presented with severe outcomes in >50% of the population when infected with H1N1pdm09.[10] This is not in line with what was observed clinically in the aged human population for this influenza strain, however, this difference is accounted for by pre-existing immunity to an ancestor of the H1N1pdm09 strain.[4,6] In general, aged populations are known to have more severe outcomes upon infection with influenza A viruses.[30,31]

We analyzed the baseline expression level of host glycans prior to influenza virus infection in lung punch biopsies from newly weaned (NW, n=6), adult (AD, n=4) and aged ferrets (AG, n=3) using our dual-color lectin microarray technology (**Scheme 1**).[25,26] Biopsies from both the upper and lower lobes were analyzed for each ferret. Lectin microarrays utilize carbohydrate-binding proteins with well-defined specificities to detect glycan changes between samples.[22,25-27] In brief, frozen tissue samples were sonicated and labeled with either Alexa Fluor 555-NHS (sample), or Alexa Fluor 647-NHS (reference). A pooled reference consisting of all samples was used. Equal amounts of sample and reference were analyzed on the lectin microarrays (>100 probes, **Supplementary Table 1**). A heatmap of the normalized data, ordered by ferret age, is shown in **Figure 1a**.

Sialic acid glycoconjugates on the host cell surface play a crucial role as both the receptor for influenza binding by hemagglutinin (α-2,6-sialosides) and as the target of the influenza neuraminidase (α-2,3- and α-2,6 sialosides). Differences in sialoside levels may play a role in

6

differential susceptibility to the virus with age. In light of this we examined the expression level of α-2,3- and α-2,6-sialosides in the ferret lung. Both newly weaned and aged ferret lungs had higher levels of α-2,6-sialosides than adult lungs (lectins: SNA, TJA-I, ~ 1.3-fold NW:AD, ~1.4-fold AG:AD, **Figure 1b** and **Supplementary Figure S1**), indicating that they may be more susceptible to viral infection. In contrast to α-2,6-sialic acid, we observed a significant age-dependent decrease in α-2,3-sialosides (lectin: MAL-II (~1.5-fold NW:AD, ~2-fold NW:AG), SLBR-N,[32] diCBM40, SLBR-H,[32] **Figure 1c** and **Supplementary Figure S2**). Of particular note, the lectin MAL-II mainly recognizes α-2,3-sialic acids on *O*-linked glycans. These glycans commonly decorate proteins such as mucins, whose heavily sialylated structures often act as a trap for viral particles.[33] While a decrease in α-2,3-sialosides is observed with age, we also observe an increase in mucin levels in the lungs (Antibodies: MUC5AC, MUC15, **Supplementary Figure S3**). In addition, we observe a potentially related increase in Lewis structures (Le), which are often observed on mucins (Antibodies: Le[b], Le[x], Le[y], **Supplementary Figure S4**). Taken together, this suggests that the protective, highly sialylated mucins,[34-36] that allow clearance of the virus from the lungs, may alter with age in a way that diminishes their protective capacity. This data correlates well with the differences in viral clearance observed in these ferrets, with young ferrets showing more rapid clearance and aged ferrets showing prolonged infection and lower clearance of the virus upon infection.[10]

Recently our group identified high mannose as a severity marker for influenza H1N1pdm09 infection in adult ferrets.[19] High mannose, defined here as Man$_{7-9}$, and oligo-mannose (defined as Man$_{5-7}$) are targets for innate immune lectin binding and may play a direct role in the damage observed in influenza. Analysis of the mannose binding lectins on the array showed distinct profiles for levels of high- and oligo-mannose.[37] Uninfected newly weaned animals had

7

significantly lower levels of oligo-mannose (GNL, NPA, HHL, **Figure 1d** and **Supplementary Figure S5**) than either adult or aged ferrets. However, high-mannose levels, recognized by the anti-viral lectin Griffithsin (GRFT),[38] were higher in the newly weaned and adult animals as compared to the aged ferrets. Whether age-dependent differences in the baseline levels of mannose in uninfected animals have any bearing on the levels of the host response to influenza is currently unclear.

Aged ferrets have a distinct glycomic response from adults to influenza infection.

Disease progression in adult and aged ferrets infected with H1N1pdm09 differ dramatically in timing and presentation.[10] Aged ferrets had more persistent viral infections and were unable to clear the virus by day 8 post-infection, in contrast to adults. They also developed pneumonia later in the course of their illness and had higher rates of mortality. To study the impact of glycosylation on the host response to influenza in the aged population, we performed lectin microarray analysis on lung punch biopsies from infected aged ferrets (age > 5.5 years). We performed two concurrent studies, a severity study at day 8 post-infection (dpi 8, n = 29 ferrets) and a time-course analysis that included the day 8 samples (dpi 1: n = 5; dpi 3: n = 7; dpi 5: n = 12 ferrets, **Scheme 2**). Uninfected aged ferrets were used as a control (n=3 ferrets). We analyzed 2 samples for each ferret.

The animals analyzed in this study correspond to the animals for which pathology data was obtained in Bissel et al.[10] In our previous work, weight loss was used to evaluate the severity of illness.[10, 19] This is a common metric for severity in animal models and can only be used for timepoints > day 5 post-infection. In studying the disease progression in aged ferrets we observed a disparity between the pathology and the weight loss data. In this age group, a severe outcome by weight loss was defined as >20% loss of mass.[10] A pneumonia composite score (PCS), which sums the scores for lung involvement, bronchial severity, and alveolar severity was used to evaluate

severity by pathology.[10] In aged animals, which present with pneumonia at later stages of infection, degree of severity by pathology cannot be determined for early timepoints. A comparison of the severity as defined by weight loss quartiles (Q0-Q1:<18.3%, Q1-Q3: 18.3%-21.9%, Q3-Q4: >21.9%, **Supplementary Figure S6**) to the pneumonia composite scores at day 8 showed no concordance between the two metrics. Instead, in the aged population the trend was towards lower weight loss with increased severity by pathology. This is in direct opposition to the trend observed in adult ferrets. Based on our analysis, weight loss was not an appropriate metric for severity in aged ferrets. Thus, the pneumonia composite score was used as the severity metric for this cohort, as it represents the physiologically relevant degree of illness in influenza infection. We used quartiles to define mild, moderate, and severe infections in the aged population (Mild: PCS < 8.5, n=6 ferrets; Moderate: PCS = 8.5-11, n=15; Severe: PCS > 11, n=8). A heatmap of the normalized data for ferrets sacrificed at day 7-8 post-infection arranged by severity is presented in **Figure 2**. A heatmap of the time-course analysis for aged ferrets is shown in **Supplementary Figure S7**.

We observed several changes in aged ferrets as a function of infection that did not overlay onto severity. For ease of comparison between the aged and adult host-responses, we reanalyzed the lectin microarray data from our adult ferret cohort[19] using PCS as the severity metric. In our previous work, adult ferrets showed an increase in α-2,6 sialylation at early infection timepoints, with levels returning to baseline by day 8 post-infection. In contrast, we see a significant loss of α-2,6 sialylation in the aged ferret lungs with this loss occurring early in the course of infection (SNA, TJA-I, **Figure 2** and **Supplementary Figure S8**). We also observe a loss in α-2,3-sialosides by day 8 post-infection in aged animals (SLBR-B, SLBR-H, SLBR-N, diCBM-40, MAL-I, MAL-II, **Figure 2** and **Supplementary Figure S9**). A similar loss of α-2,3-sialosides was observed in adult ferrets. However, in this population, the response was immediate, while in the aged animals

9

a more gradual loss of this glycan was observed. Influenza neuraminidases are known to prefer α-2,3-sialosides,[39,40] and the more gradual loss of this glycan in aged ferrets maps onto the pattern of delayed infection observed in the lungs.[10]

Uninfected aged animals had higher levels of non-sialylated mucins compared to adults. Upon infection, we observed a substantial loss of *O*-linked glycans, Lewis structures, and mucins in aged ferrets (AIA, HAA, HPA, MPA, MNA-G, Mucin 15, Le[a], Le[b], Le[y], **Figure 2** and **Supplementary Figure S10**). This is similar to previous observations made in adult ferrets, however, the degree of host response in the aged ferrets was more pronounced. We observed a strong loss of *O*-linked glycans, Lewis structures and mucins at the earliest time points (**Supplementary Figure S11**), which may contribute to the inability of older animals to effectively fight infection.

Our previous work suggested a role for high/oligo-mannose as a key mediator of influenza severity.[19] In our original analysis, severity in the adult ferrets was defined by weight loss. Re-analysis of this data using pneumonia composite scores did not change the previously observed relationship between high/oligo-mannose levels and severity **(Supplementary Figure S12)**. We observe a similar increase in high mannose as a function of severity in the aged animals when severity is defined by pathology (GRFT, HHL, H84T,[41] NPA, GNA, ASA, **Figures 2** and **Figure 3** and **Supplementary Figure S12**). However, the timing of high mannose induction in the aged ferrets is delayed when compared to adults. In the adult ferrets, high mannose was induced at day 1 post-infection in line with the damage observed by pathology.[10] In the aged ferrets, we observe significant changes in high mannose by day 3, which persisted to day 8 post-infection. This is consistent with the more delayed development of pneumonia in these animals. Overall, this data supports high mannose as a marker and potential mediator of severity in the host response to influenza infection.

Newly weaned ferrets show no severity-dependent changes in the glycome.

The 2019 pandemic H1N1 virus presented with mild clinical symptoms in young children.[42-44] H1N1pdm09 infection in newly weaned ferrets mimic these clinical symptoms, with lower fevers and less weight loss.[9] Newly weaned ferrets clear virus faster and have much lower levels of alveolar pneumonia.[10] We analyzed the glycosylation changes in the lungs of newly weaned ferrets (6-7 weeks) infected with H1N1pdm09 for which we had previously obtained pathology data.[10] To examine the changes in glycosylation over the course of the infection, we performed a time-course study (uninfected, n = 16; dpi 3, n = 4; dpi 5, n = 4; dpi 8, n = 42; dpi 14, n = 3, 2 samples per ferret). Severity was determined for day 8 samples using the PCS metric as previously described. A heatmap of the time-course data, organized by severity for day 8 post-infection, is shown in **Figure 4**.

In contrast to both adults and aged ferrets, we saw no clear severity-dependent differences in the newly weaned animals at day 8 post-infection. We did observe an increase in complex N-glycan epitopes early in the course of infection, peaking by day 5 and returning to pre-infection levels by day 8 (α-2,6-sialic acid: SNA; core fucose: LcH, PSA; bisecting branching: PHA-E, Calsepa, **Figure 4** and **Supplementary Figure S13**). Although high/oligo-mannose trended with complex N-glycans in the time-course, the changes were not statistically significant. Overall, the lack of strong changes in the glycome is consistent with the mild nature of illness observed in young ferrets, modeling the human population.

CONCLUSIONS

11

In 2009, a new pandemic H1N1 influenza A virus emerged and displayed an unusual severity pattern, impacting adults more severely than young children or the elderly. The lower impact on the elderly population, who are typically at high-risk for influenza severity, was later determined to be a result of pre-existing immunity. The ferret model of influenza has been found to mimic the differences in age-dependent illness observed in the absence of pre-existing immunity. In this model, there is a gradient of severity with young ferrets showing mild illness and aged ferrets displaying high severity. The origins of this disparity in host response is still unclear. In this work, we show dramatic age-dependent differences in the ferret glycome and host-response to influenza that overlay differences observed in severity. These include age-dependent differences in mucin-related epitopes that may explain differences in viral clearance observed between populations. In previous work, we posited that the induction of high-mannose due to influenza infection could be causative of severity through over-engagement of the innate immune system via lectins, such as MBL2. Our current study shows that high-mannose is induced in the aged population, where high levels of severity are observed, but not in newly weaned ferrets, which display a mild phenotype. This is consistent with our hypothesis and points to the need for further study to determine if the glycomic host response is a critical mediator of influenza severity.

ASSOCIATED CONTENT

Supporting Information.

Boxplots of α-2,6-sialoside signal by age in uninfected ferrets; Boxplots of α-2,3-sialoside levels by age in uninfected ferrets; Boxplots of mucins expressions by age in uninfected ferrets; Boxplots of Lewis structures by age in uninfected ferrets; Boxplots of high/oligo-mannose levels by age in uninfected ferrets; Boxplots of Pneumonia Composite Score (PCS) as a function of weight loss

quartiles in adult and aged ferrets; Aged ferrets had delayed response to influenza infection; Impact of influenza infection on α-2,6-sialosides in adult and aged ferrets; Impact of influenza infection on α-2,3-sialosides in adult and aged ferrets; Impact of influenza infection on *O*-linked glycans in aged ferrets; Dynamic changes in *O*-linked glycans are observed upon infection in aged ferrets; Comparison of severity metrics used in adult and aged ferrets; Glycan changes are observed early in the time-course study of newly weaned ferrets; Lectins used in microarrays. (PDF)

AUTHOR INFORMATION

Corresponding Author

***Lara K. Mahal**-*Canada Excellence Research Chair in Glycomics, Department of Chemistry, University of Alberta, Edmonton, Alberta, T6G 2G2, CANADA*. orcid.org/0000-0003-4791-8524; Phone: 780-492-5847; Email: lkmahal@ualberta.ca

 Authors

Shuhui Chen- *Biomedical Research Institute, Department of Chemistry, New York University, NY, 10003, USA*

Brian Kasper- *Biomedical Research Institute, Department of Chemistry, New York University, NY, 10003, USA*

Bin Zhang- *Department of Genetics and Genomic Sciences, Mount Sinai Center for Transformative Disease Modeling, Icahn Institute of Genomics and Multiscale Biology, Icahn School of Medicine at Mount Sinai, NY, 10029, USA*

Lauren P. Lashua- *Center for Genomics & Systems Biology, Department of Biology, New York University, NY, 10003, USA*

Ted M. Ross- *Center for Vaccines and Immunology, University of Georgia, GA, 30602, USA*

Elodie Ghedin- *Center for Genomics & Systems Biology, Department of Biology and Department of Epidemiology, School of Global Public Health, New York University, NY, 10003, USA.*

ACKNOWLEDGMENT

REFERENCES

1. Iuliano, A. D.; Roguski, K. M.; Chang, H. H.; Muscatello, D. J.; Palekar, R.; Tempia, S.; Cohen, C.; Gran, J. M.; Schanzer, D.; Cowling, B. J.; Wu, P.; Kyncl, J.; Ang, L. W.; Park,

M.; Redlberger-Fritz, M.; Yu, H.; Espenhain, L.; Krishnan, A.; Emukule, G.; van Asten, L.; Pereira da Silva, S.; Aungkulanon, S.; Buchholz, U.; Widdowson, M.-A.; Bresee, J. S.; Azziz-Baumgartner, E.; Cheng, P.-Y.; Dawood, F.; Foppa, I.; Olsen, S.; Haber, M.; Jeffers, C.; MacIntyre, C. R.; Newall, A. T.; Wood, J. G.; Kundi, M.; Popow-Kraupp, T.; Ahmed, M.; Rahman, M.; Marinho, F.; Sotomayor Proschle, C. V.; Vergara Mallegas, N.; Luzhao, F.; Sa, L.; Barbosa-Ramírez, J.; Sanchez, D. M.; Gomez, L. A.; Vargas, X. B.; Acosta Herrera, a.; Llanés, M. J.; Fischer, T. K.; Krause, T. G.; Mølbak, K.; Nielsen, J.; Trebbien, R.; Bruno, A.; Ojeda, J.; Ramos, H.; an der Heiden, M.; del Carmen Castillo Signor, L.; Serrano, C. E.; Bhardwaj, R.; Chadha, M.; Narayan, V.; Kosen, S.; Bromberg, M.; Glatman-Freedman, A.; Kaufman, Z.; Arima, Y.; Oishi, K.; Chaves, S.; Nyawanda, B.; Al-Jarallah, R. A.; Kuri-Morales, P. A.; Matus, C. R.; Corona, M. E. J.; Burmaa, A.; Darmaa, O.; Obtel, M.; Cherkaoui, I.; van den Wijngaard, C. C.; van der Hoek, W.; Baker, M.; Bandaranayake, D.; Bissielo, A.; Huang, S.; Lopez, L.; Newbern, C.; Flem, E.; Grøneng, G. M.; Hauge, S.; de Cosío, F. G.; de Moltó, Y.; Castillo, L. M.; Cabello, M. A.; von Horoch, M.; Medina Osis, J.; Machado, A.; Nunes, B.; Rodrigues, A. P.; Rodrigues, E.; Calomfirescu, C.; Lupulescu, E.; Popescu, R.; Popovici, O.; Bogdanovic, D.; Kostic, M.; Lazarevic, K.; Milosevic, Z.; Tiodorovic, B.; Chen, M.; Cutter, J.; Lee, V.; Lin, R.; Ma, S.; Cohen, A. L.; Treurnicht, F.; Kim, W. J.; Delgado-Sanz, C.; de mateo Ontañón, S.; Larrauri, A.; León, I. L.; Vallejo, F.; Born, R.; Junker, C.; Koch, D.; Chuang, J.-H.; Huang, W.-T.; Kuo, H.-W.; Tsai, Y.-C.; Bundhamcharoen, K.; Chittaganpitch, M.; Green, H. K.; Pebody, R.; Goñi, N.; Chiparelli, H.; Brammer, L.; Mustaquim, D., Estimates of global seasonal influenza-associated respiratory mortality: a modelling study. *The Lancet* **2018,** *391* (10127), 1285-1300.

2.   Medina, R. A.; Garcia-Sastre, A., Influenza A viruses: new research developments. *Nat Rev Microbiol* **2011,** *9* (8), 590-603.

3.   Chowell, G.; Bertozzi, S. M.; Colchero, M. A.; Lopez-Gatell, H.; Alpuche-Aranda, C.; Hernandez, M.; Miller, M. A., Severe respiratory disease concurrent with the circulation of H1N1 influenza. *N Engl J Med* **2009,** *361* (7), 674-9.

4.   Verma, N.; Dimitrova, M.; Carter, D. M.; Crevar, C. J.; Ross, T. M.; Golding, H.; Khurana, S., Influenza virus H1N1pdm09 infections in the young and old: evidence of greater antibody diversity and affinity for the hemagglutinin globular head domain (HA1 Domain) in the elderly than in young adults and children. *J Virol* **2012,** *86* (10), 5515-22.

5.   Hancock, K.; Veguilla, V.; Lu, X.; Zhong, W.; Butler, E. N.; Sun, H.; Liu, F.; Dong, L.; DeVos, J. R.; Gargiullo, P. M.; Brammer, T. L.; Cox, N. J.; Tumpey, T. M.; Katz, J. M., Cross-reactive antibody responses to the 2009 pandemic H1N1 influenza virus. *N Engl J Med* **2009,** *361* (20), 1945-52.

6.   Giles, B. M.; Bissel, S. J.; Craigo, J. K.; Dealmeida, D. R.; Wiley, C. A.; Tumpey, T. M.; Ross, T. M., Elicitation of anti-1918 influenza virus immunity early in life prevents morbidity and lower levels of lung infection by 2009 pandemic H1N1 influenza virus in aged mice. *J Virol* **2012,** *86* (3), 1500-13.

7.   Carter, D. M.; Darby, C. A.; Johnson, S. K.; Carlock, M. A.; Kirchenbaum, G. A.; Allen, J. D.; Vogel, T. U.; Delagrave, S.; DiNapoli, J.; Kleanthous, H.; Ross, T. M., Elicitation of Protective Antibodies against a Broad Panel of H1N1 Viruses in Ferrets Preimmune to Historical H1N1 Influenza Viruses. *J Virol* **2017,** *91* (24).

8.   Rowe, T.; Leon, A. J.; Crevar, C. J.; Carter, D. M.; Xu, L.; Ran, L.; Fang, Y.; Cameron, C. M.; Cameron, M. J.; Banner, D.; Ng, D. C.; Ran, R.; Weirback, H. K.; Wiley, C. A.; Kelvin, D. J.; Ross, T. M., Modeling host responses in ferrets during A/California/07/2009 influenza infection. *Virology* **2010,** *401* (2), 257-65.

9.   Huang, S. S.; Banner, D.; Degousee, N.; Leon, A. J.; Xu, L.; Paquette, S. G.; Kanagasabai, T.; Fang, Y.; Rubino, S.; Rubin, B.; Kelvin, D. J.; Kelvin, A. A., Differential pathological and immune responses in newly weaned ferrets are associated with a mild clinical outcome of pandemic 2009 H1N1 infection. *J Virol* **2012,** *86* (24), 13187-201.

10.   Bissel, S. J.; Carter, C. E.; Wang, G.; Johnson, S. K.; Lashua, L. P.; Kelvin, A. A.; Wiley, C. A.; Ghedin, E.; Ross, T. M., Age-Related Pathology Associated with H1N1 A/California/07/2009 Influenza Virus Infection. *Am J Pathol* **2019,** *189* (12), 2389-2399.

11.   Belser, J. A.; Katz, J. M.; Tumpey, T. M., The ferret as a model organism to study influenza A virus infection. *Dis Model Mech* **2011,** *4* (5), 575-9.

12.   Walther, T.; Karamanska, R.; Chan, R. W.; Chan, M. C.; Jia, N.; Air, G.; Hopton, C.; Wong, M. P.; Dell, A.; Malik Peiris, J. S.; Haslam, S. M.; Nicholls, J. M., Glycomic analysis of human respiratory tract tissues and correlation with influenza virus infection. *PLoS Pathog* **2013,** *9* (3), e1003223.

13.   Jia, N.; Barclay, W. S.; Roberts, K.; Yen, H. L.; Chan, R. W.; Lam, A. K.; Air, G.; Peiris, J. S.; Dell, A.; Nicholls, J. M.; Haslam, S. M., Glycomic characterization of respiratory tract tissues of ferrets: implications for its use in influenza virus infection studies. *J Biol Chem* **2014,** *289* (41), 28489-504.

14.   Nicholls, J. M., The battle between influenza and the innate immune response in the human respiratory tract. *Infect Chemother* **2013,** *45* (1), 11-21.

15.   Jia, N.; Byrd-Leotis, L.; Matsumoto, Y.; Gao, C.; Wein, A. N.; Lobby, J. L.; Kohlmeier, J. E.; Steinhauer, D. A.; Cummings, R. D., The Human Lung Glycome Reveals Novel Glycan Ligands for Influenza A Virus. *Sci Rep* **2020,** *10* (1), 5320.

16.   Cohen, M.; Zhang, X. Q.; Senaati, H. P.; Chen, H. W.; Varki, N. M.; Schooley, R. T.; Gagneux, P., Influenza A penetrates host mucus by cleaving sialic acids with neuraminidase. *Virology Journal* **2013,** *10*.

17.   Gubareva, L. V.; Kaiser, L.; Hayden, F. G., Influenza virus neuraminidase inhibitors. *The Lancet* **2000,** *355* (9206), 827-835.

18.   Moscona, A., Neuraminidase inhibitors for influenza. *N Engl J Med* **2005,** *353* (13), 1363-73.

19.   Heindel, D. W.; Koppolu, S.; Zhang, Y.; Kasper, B.; Meche, L.; Vaiana, C.; Bissel, S. J.; Carter, C. E.; Kelvin, A. A.; Zhang, B.; Zhou, B.; Chou, T.-W.; Lashua, L.; Ross, T. M.; Ghedin, E.; Mahal, L. K., **2020**.

20.   Zogheib, E.; Nyga, R.; Cornu, M.; Sendid, B.; Monconduit, J.; Jounieaux, V.; Maizel, J.; Segard, C.; Chouaki, T.; Dupont, H., Prospective Observational Study on the Association Between Serum Mannose-Binding Lectin Levels and Severe Outcome in Critically Ill Patients with Pandemic Influenza Type A (H1N1) Infection. *Lung* **2018,** *196* (1), 65-72.

21.   Ling, M. T.; Tu, W.; Han, Y.; Mao, H.; Chong, W. P.; Guan, J.; Liu, M.; Lam, K. T.; Law, H. K.; Peiris, J. S.; Takahashi, K.; Lau, Y. L., Mannose-binding lectin contributes to

deleterious inflammatory response in pandemic H1N1 and avian H9N2 infection. *J Infect Dis* **2012,** *205* (1), 44-53.

22.   Pilobello, K. T.; Krishnamoorthy, L.; Slawek, D.; Mahal, L. K., Development of a lectin microarray for the rapid analysis of protein glycopatterns. *Chembiochem* **2005,** *6* (6), 985-9.

23.   Batista, B. S.; Eng, W. S.; Pilobello, K. T.; Hendricks-Munoz, K. D.; Mahal, L. K., Identification of a conserved glycan signature for microvesicles. *J Proteome Res* **2011,** *10* (10), 4624-33.

24.   Agrawal, P.; Fontanals-Cirera, B.; Sokolova, E.; Jacob, S.; Vaiana, C. A.; Argibay, D.; Davalos, V.; McDermott, M.; Nayak, S.; Darvishian, F.; Castillo, M.; Ueberheide, B.; Osman, I.; Fenyo, D.; Mahal, L. K.; Hernando, E., A Systems Biology Approach Identifies FUT8 as a Driver of Melanoma Metastasis. *Cancer Cell* **2017,** *31* (6), 804-819 e7.

25.   Pilobello, K. T.; Slawek, D. E.; Mahal, L. K., A ratiometric lectin microarray approach to analysis of the dynamic mammalian glycome. *Proc Natl Acad Sci U S A* **2007,** *104* (28), 11534-9.

26.   Pilobello, K. T.; Agrawal, P.; Rouse, R.; Mahal, L. K., Advances in lectin microarray technology: optimized protocols for piezoelectric print conditions. *Curr Protoc Chem Biol* **2013,** *5* (1), 1-23.

27.   Koppolu, S.; Wang, L.; Mathur, A.; Nigam, J. A.; Dezzutti, C. S.; Isaacs, C.; Meyn, L.; Bunge, K. E.; Moncla, B. J.; Hillier, S. L.; Rohan, L. C.; Mahal, L. K., Vaginal Product Formulation Alters the Innate Antiviral Activity and Glycome of Cervicovaginal Fluids with Implications for Viral Susceptibility. *ACS Infect Dis* **2018,** *4* (11), 1613-1622.

28.   Clohisey, S.; Baillie, J. K., Host susceptibility to severe influenza A virus infection. *Crit Care* **2019,** *23* (1), 303.

29.   Czaja, C. A.; Miller, L.; Alden, N.; Wald, H. L.; Cummings, C. N.; Rolfes, M. A.; Anderson, E. J.; Bennett, N. M.; Billing, L. M.; Chai, S. J.; Eckel, S.; Mansmann, R.; McMahon, M.; Monroe, M. L.; Muse, A.; Risk, I.; Schaffner, W.; Thomas, A. R.; Yousey-Hindes, K.; Garg, S.; Herlihy, R. K., Age-Related Differences in Hospitalization Rates, Clinical Presentation, and Outcomes Among Older Adults Hospitalized With Influenza-U.S. Influenza Hospitalization Surveillance Network (FluSurv-NET). *Open Forum Infect Dis* **2019,** *6* (7).

30.   Zhang, A. J.; To, K. K.; Tse, H.; Chan, K. H.; Guo, K. Y.; Li, C.; Hung, I. F.; Chan, J. F.; Chen, H.; Tam, S.; Yuen, K. Y., High incidence of severe influenza among individuals over 50 years of age. *Clin Vaccine Immunol* **2011,** *18* (11), 1918-24.

31.   Caini, S.; Spreeuwenberg, P.; Kusznierz, G. F.; Rudi, J. M.; Owen, R.; Pennington, K.; Wangchuk, S.; Gyeltshen, S.; Ferreira de Almeida, W. A.; Pessanha Henriques, C. M.; Njouom, R.; Vernet, M. A.; Fasce, R. A.; Andrade, W.; Yu, H.; Feng, L.; Yang, J.; Peng, Z.; Lara, J.; Bruno, A.; de Mora, D.; de Lozano, C.; Zambon, M.; Pebody, R.; Castillo, L.; Clara, A. W.; Matute, M. L.; Kosasih, H.; Nurhayati; Puzelli, S.; Rizzo, C.; Kadjo, H. A.; Daouda, C.; Kiyanbekova, L.; Ospanova, A.; Mott, J. A.; Emukule, G. O.; Heraud, J. M.; Razanajatovo, N. H.; Barakat, A.; El Falaki, F.; Huang, S. Q.; Lopez, L.; Balmaseda, A.; Moreno, B.; Rodrigues, A. P.; Guiomar, R.; Ang, L. W.; Lee, V. J. M.; Venter, M.; Cohen, C.; Badur, S.; Ciblak, M. A.; Mironenko, A.; Holubka, O.; Bresee, J.; Brammer, L.; Hoang, P. V. M.; Le, M. T. Q.; Fleming, D.; Seblain, C. E.; Schellevis, F.; Paget, J.; Global Influenza, B. S. g., Distribution of

influenza virus types by age using case-based global surveillance data from twenty-nine countries, 1999-2014. *BMC Infect Dis* **2018,** *18* (1), 269.

32.   Bensing, B. A.; Li, Q.; Park, D.; Lebrilla, C. B.; Sullam, P. M., Streptococcal Siglec-like adhesins recognize different subsets of human plasma glycoproteins: implications for infective endocarditis. *Glycobiology* **2018,** *28* (8), 601-611.

33.   Ridley, C.; Thornton, D. J., Mucins: the frontline defence of the lung. *Biochem Soc Trans* **2018,** *46* (5), 1099-1106.

34.   Lillehoj, E. P.; Kato, K.; Lu, W.; Kim, K. C., Cellular and molecular biology of airway mucins. *Int Rev Cell Mol Biol* **2013,** *303*, 139-202.

35.   Delaveris, C. S.; Webster, E. R.; Banik, S. M.; Boxer, S. G.; Bertozzi, C. R., Membrane-tethered mucin-like polypeptides sterically inhibit binding and slow fusion kinetics of influenza A virus. *Proc Natl Acad Sci U S A* **2020**.

36.   Zanin, M.; Baviskar, P.; Webster, R.; Webby, R., The Interaction between Respiratory Pathogens and Mucus. *Cell Host Microbe* **2016,** *19* (2), 159-68.

37.   Wong, M. Y.; Chen, K.; Antonopoulos, A.; Kasper, B. T.; Dewal, M. B.; Taylor, R. J.; Whittaker, C. A.; Hein, P. P.; Dell, A.; Genereux, J. C.; Haslam, S. M.; Mahal, L. K.; Shoulders, M. D., XBP1s activation can globally remodel N-glycan structure distribution patterns. *Proc Natl Acad Sci U S A* **2018,** *115* (43), E10089-E10098.

38.   Mori, T.; O'Keefe, B. R.; Sowder, R. C., 2nd; Bringans, S.; Gardella, R.; Berg, S.; Cochran, P.; Turpin, J. A.; Buckheit, R. W., Jr.; McMahon, J. B.; Boyd, M. R., Isolation and

characterization of griffithsin, a novel HIV-inactivating protein, from the red alga Griffithsia sp. *J Biol Chem* **2005,** *280* (10), 9345-53.

39.   Air, G. M., Influenza neuraminidase. *Influenza Other Respir Viruses* **2012,** *6* (4), 245-56.

40.   Gerlach, T.; Kuhling, L.; Uhlendorff, J.; Laukemper, V.; Matrosovich, T.; Czudai-Matwich, V.; Schwalm, F.; Klenk, H. D.; Matrosovich, M., Characterization of the neuraminidase of the H1N1/09 pandemic influenza virus. *Vaccine* **2012,** *30* (51), 7348-52.

41.   Swanson, M. D.; Boudreaux, D. M.; Salmon, L.; Chugh, J.; Winter, H. C.; Meagher, J. L.; Andre, S.; Murphy, P. V.; Oscarson, S.; Roy, R.; King, S.; Kaplan, M. H.; Goldstein, I. J.; Tarbet, E. B.; Hurst, B. L.; Smee, D. F.; de la Fuente, C.; Hoffmann, H. H.; Xue, Y.; Rice, C. M.; Schols, D.; Garcia, J. V.; Stuckey, J. A.; Gabius, H. J.; Al-Hashimi, H. M.; Markovitz, D. M., Engineering a therapeutic lectin by uncoupling mitogenicity from antiviral activity. *Cell* **2015,** *163* (3), 746-58.

42.   Helferty, M.; Vachon, J.; Tarasuk, J.; Rodin, R.; Spika, J.; Pelletier, L., Incidence of hospital admissions and severe outcomes during the first and second waves of pandemic (H1N1) 2009. *CMAJ* **2010,** *182* (18), 1981-7.

43.   Martic, J.; Savic, N.; Minic, P.; Pasic, S.; Nedeljkovic, J.; Jankovic, B., Novel H1N1 influenza in neonates: from mild to fatal disease. *J Perinatol* **2011,** *31* (6), 446-8.

44.   Halasa, N. B., Update on the 2009 pandemic influenza A H1N1 in children. *Curr Opin Pediatr* **2010,** *22* (1), 83-7.

Abstract Figure

Sample-Alexa Fluor 555-NHS

a. Harvest lung   b. Isolate proteins   c. Label proteins   d. Analyze on lectin microarrays

Reference-Alexa Fluor 647-NHS
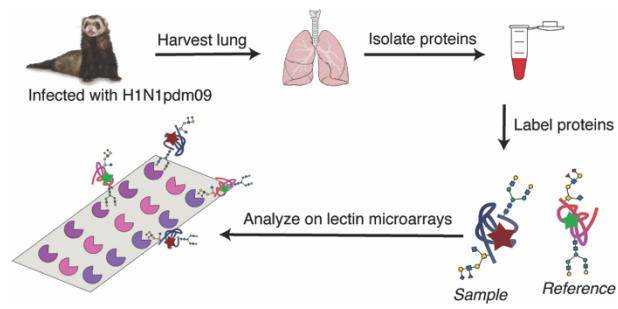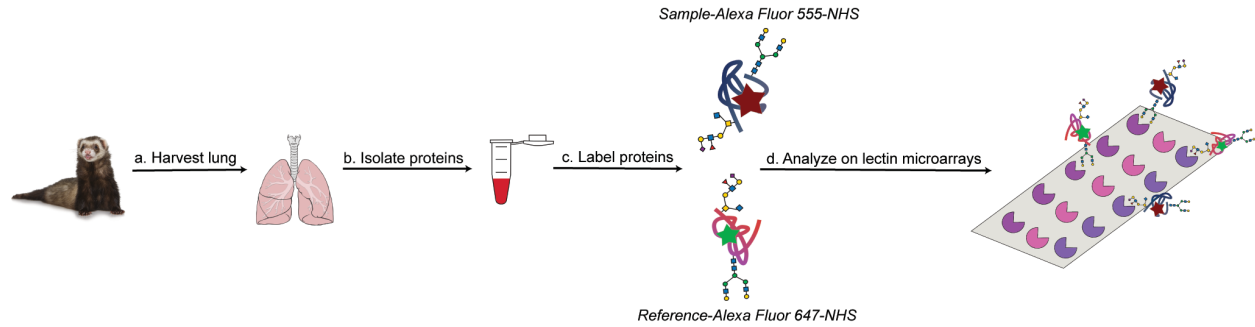
Scheme 1. Workflow of sample preparation for dual-color lectin microarray analysis. a) Lungs were harvested from ferrets infected with H1N1pdm09 and controls. b) Glycoproteins were isolated from tissues and c) labeled with Alexa Fluor 555-NHS. A pooled reference sample was orthogonally labeled with Alexa Fluor 647-NHS. d) Equal amounts of sample and reference were mixed and analyzed on lectin microarrays.
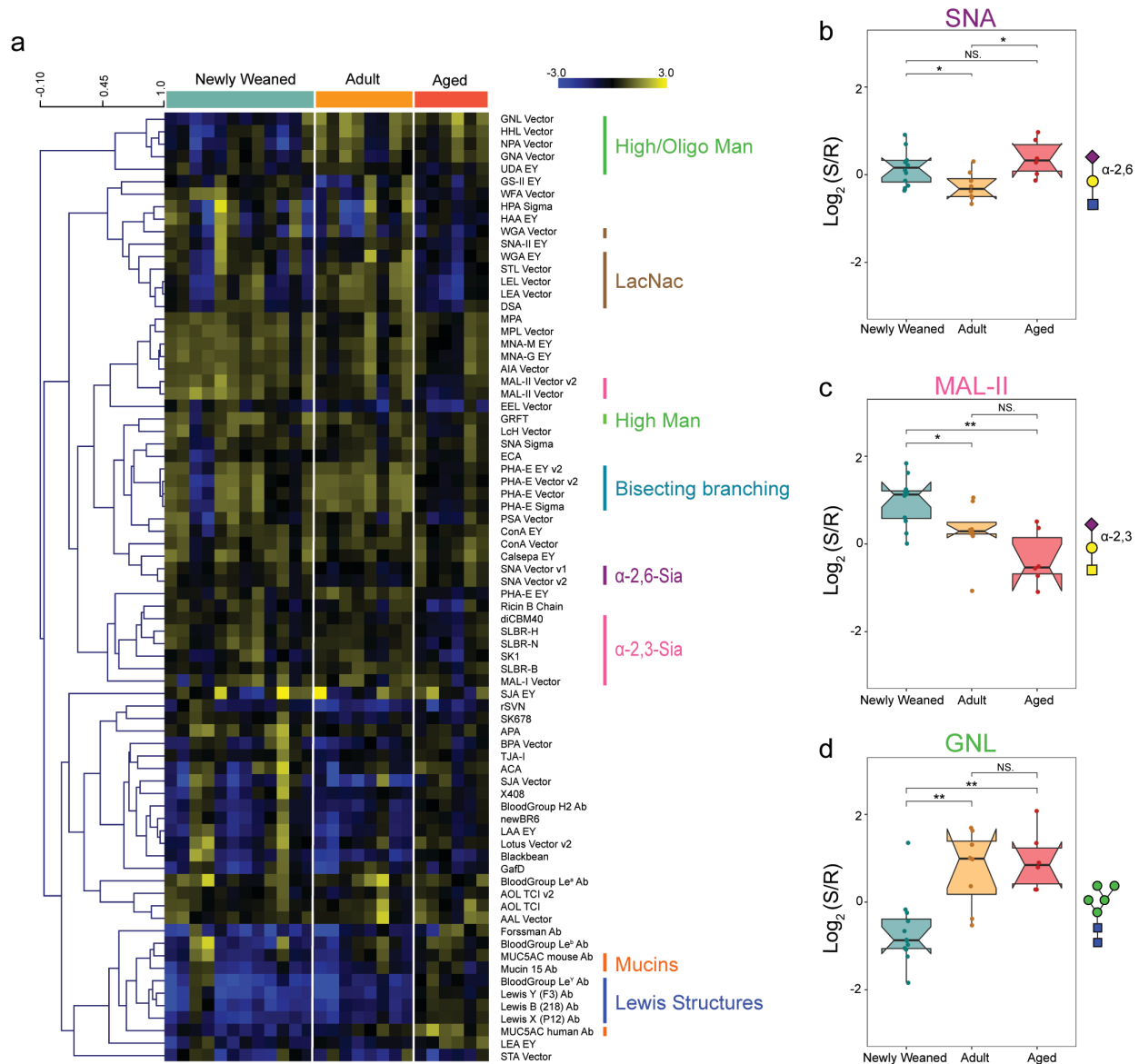
Figure 1. Baseline comparisons between different age groups of uninfected ferrets. a) Heat map of lectin microarray data. Median normalized $\log_2$ ratios (Sample (S)/Reference(R)) of ferret lung samples were ordered by age (Newly weaned, n = 6 , 2 samples per ferret; Adult, n = 4 , 2 samples per ferret; Aged, n = 3 , 2 samples per ferret). Yellow, $\log_2(S) > \log_2(R)$; blue, $\log_2(R) > \log_2(S)$. Lectins binding α-2,3-sialosides (pink), α-2,6-sialosides (purple), high/oligo-mannose (green), bisecting branching (turquoise), N-Acetyl-D-Lactosamine (brown), mucins (orange) and Lewis structures (blue) are highlighted to the right of the heatmap. b) Boxplot analysis of lectin binding by SNA (α-2,6-sialosides). c) Boxplot analysis of lectin binding by MAL-II (α-2,3-sialosides). d) Boxplot analysis of lectin binding by GNL (oligo-mannose) as a function of age. Newly weaned: cyan; Adult: orange; Aged: red. NS.: Not statistical; *: $p<0.05$; **: $p<0.01$; ***: $p<0.001$. Wilcoxon's t-test. Glycans bound by lectins are shown in the Symbolic Nomenclature for Glycomics (SNFG) at the side of the boxplots.

3

a. Collect lung tissues for lectin microarrays

Uninfected Day 1 * Day 3 Day 5 Day 8 Day 14 **

Infected with H1N1pdm09

b. Define Severity by PCS quartiles

Mild (Q0-Q1) Moderate (Q1-Q3) Severe (Q3-Q4)
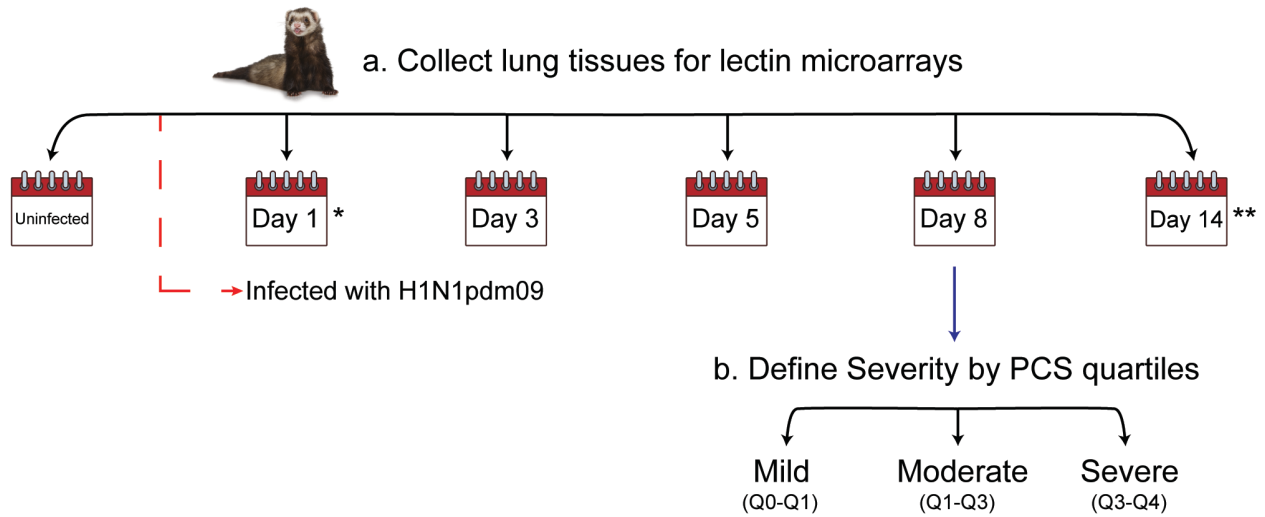
Scheme 2. Workflow of lung tissues for time-course study and severity analysis. a) Lung tissues for aged and newly weaned ferrets were collected. Lung tissues were harvested at different time points post-infection with H1N1pdm09 for lectin microarray analysis. *Day 1 time point was not collected for newly weaned ferrets. **Aged animals were sacrificed at day 8 due to weight loss >20%. b) Severity was defined by Pneumonia Composite Score (PCS) quartiles for each age group at day 8 post-infections.
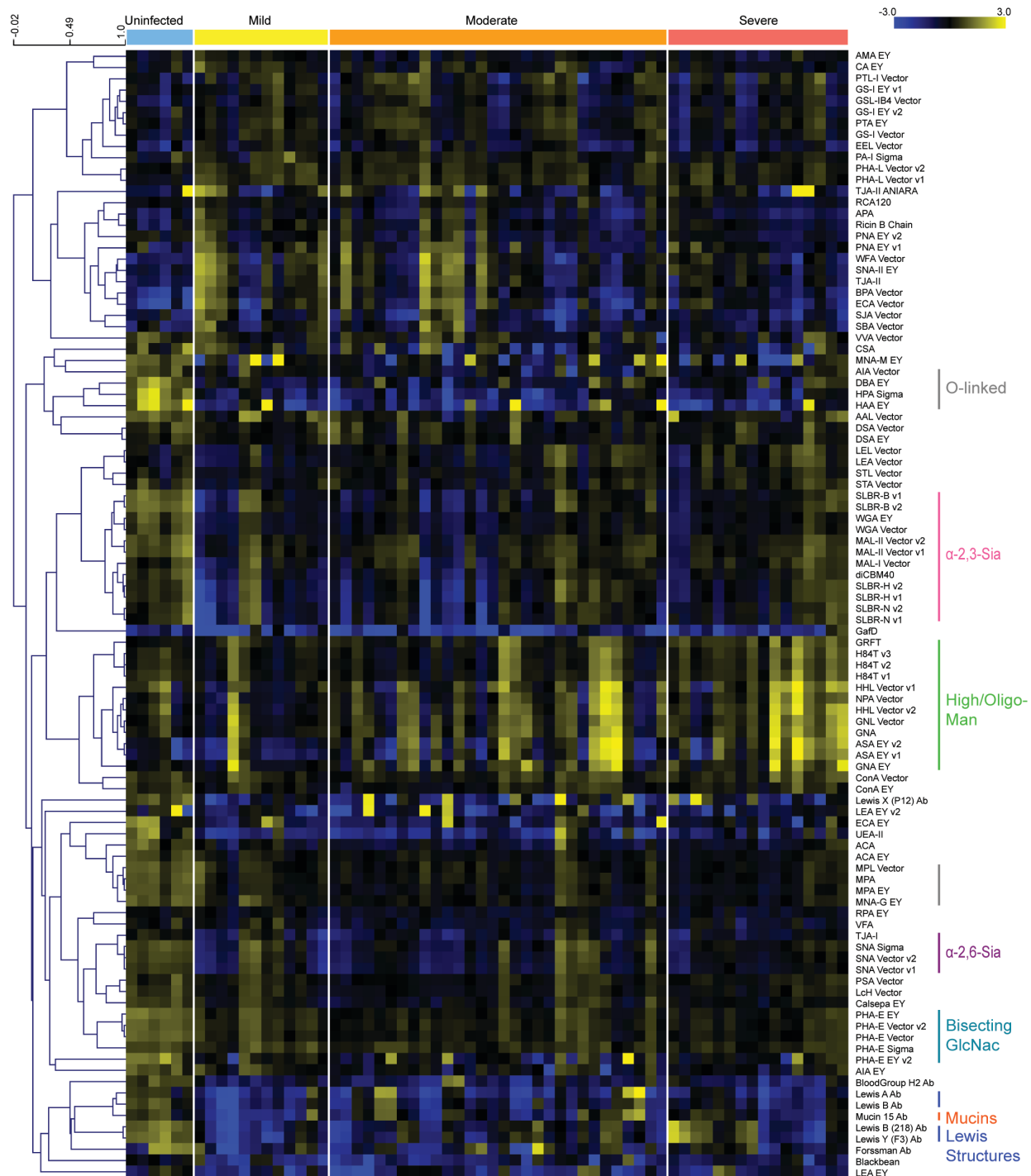
Figure 2. Glycomic changes in aged ferrets in response to influenza infection. Heat map of lectin microarray data for aged ferrets (>5.5 years) infected with H1N1pdm09. Median normalized $\log_2$ ratios (Sample (S)/Reference(R)) of ferret lung samples were ordered by severity. Uninfected (blue): n = 3. DPI 8: Mild (yellow), n = 6; Moderate (orange), n = 15; Severe (red), n = 8. 2 samples per ferret. Yellow, $\log_2(S) > \log_2(R)$; Blue, $\log_2(R) > \log_2(S)$. Lectins binding α-2,3-sialosides (pink), α-2,6-sialosides (purple), high/oligo-mannose (green), bisecting GlcNac (turquoise), *O*-linked glycans (charcoal) and Lewis structures (blue) are highlighted to the right of the heatmap.
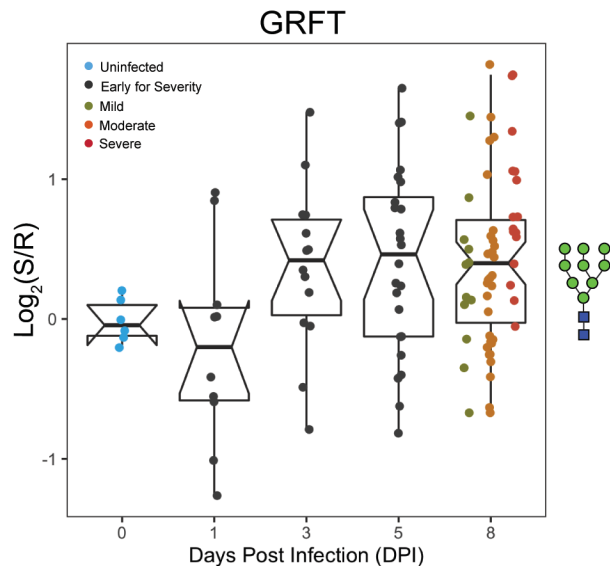
Figure 3. Dynamic changes in high-mannose are observed upon infection in aged ferrets. Time-course analysis of high-mannose as observed by GRFT following H1N1pdm09 infection (t = 0, 1, 3, 5 and 8 days). Boxplot of median normalized $\log_2$ ratios (Sample (S)/Reference(R)) is shown. Disease severity is indicated by color (Uninfected: blue; Early for Severity: black; Mild: dark yellow; Moderate: orange, Severe: red). Glycans bound by GRFT are shown in the Symbolic Nomenclature for Glycomics (SNFG) at the side of the boxplots.
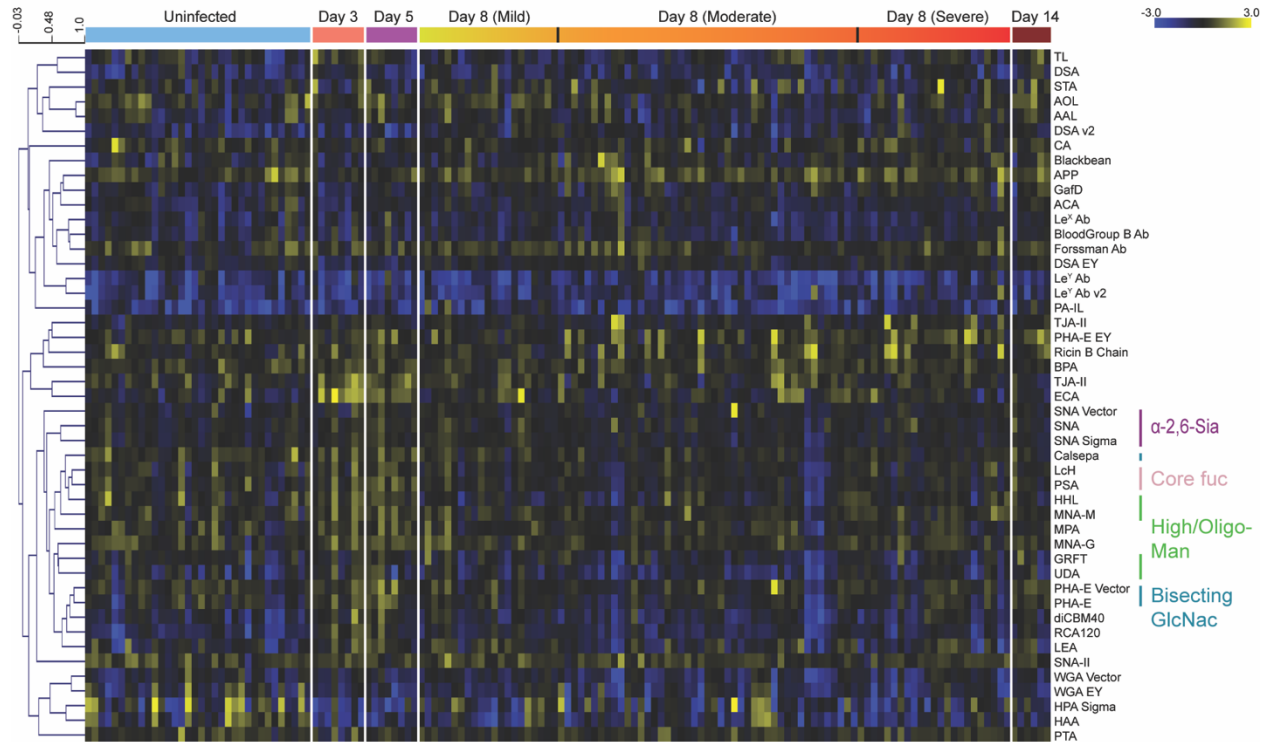
Figure 4. Newly weaned ferrets undergo glycan changes early in response to influenza. Median normalized $\log_2$ ratios (Sample (S)/Reference(R)) of newly weaned (6-7 weeks of age) ferret lung samples were ordered by days post infection. Uninfected (blue), n = 16, 2 samples per ferret; day 3 (salmon), n = 4, 2 samples per ferret; day 5 (magenta), n = 4, 2 samples per ferret; day 8, ordered by severity (mild, yellow; moderate, orange; severe, red), n = 42, 2 samples per ferret; day 14 (maroon), n = 3, 2 samples per ferret. Yellow, $\log_2(S) > \log_2(R)$; blue, $\log_2(R) > \log_2(S)$. Lectins binding α-2,6-sialosides (purple), high/oligo-mannose (green), bisecting GlcNac (turquoise), and core fucose (light pink) are highlighted to the right of the heatmap.

Supporting Information

Age-dependent glycomic response to the 2009 pandemic H1N1 influenza virus and its association with disease severity

Shuhui Chen[1], Brian Kasper[1], Bin Zhang[3], Lauren P. Lashua[4], Ted M. Ross[2], Elodie Ghedin[4,5] and Lara K. Mahal[1,6¥]

[1]Biomedical Research Institute, Department of Chemistry, New York University, NY;

[2]Center for Vaccines and Immunology, University of Georgia, GA;

[3]Department of Genetics and Genomic Sciences, Mount Sinai Center for Transformative Disease Modeling, Icahn Institute of Genomics and Multiscale Biology, Icahn School of Medicine at Mount Sinai, NY;

[4]Center for Genomics & Systems Biology, Department of Biology, New York University, NY;

[5]Department of Epidemiology, School of Global Public Health, New York University, NY;

[6]Department of Chemistry, University of Alberta, Edmonton, AB, CANADA.

¥Corresponding author: lkmahal@ualberta.ca

Table of Contents

Supplementary Figure S1. Boxplots of α-2,6-sialoside signal by age in uninfected ferrets. Boxplots of binding by α2,6-sialic acid lectins (SNA and TJA-I). Median normalized $\log_2$ ratios (Sample (S)/Reference(R)) are plotted by age (Newly weaned: cyan; Adult: orange; Aged: red). P-value from Wilcoxon's t-test is shown for indicated pairs. Glycans bound by lectins are shown in the Symbolic Nomenclature for Glycomics (SNFG) at the side of the boxplots.
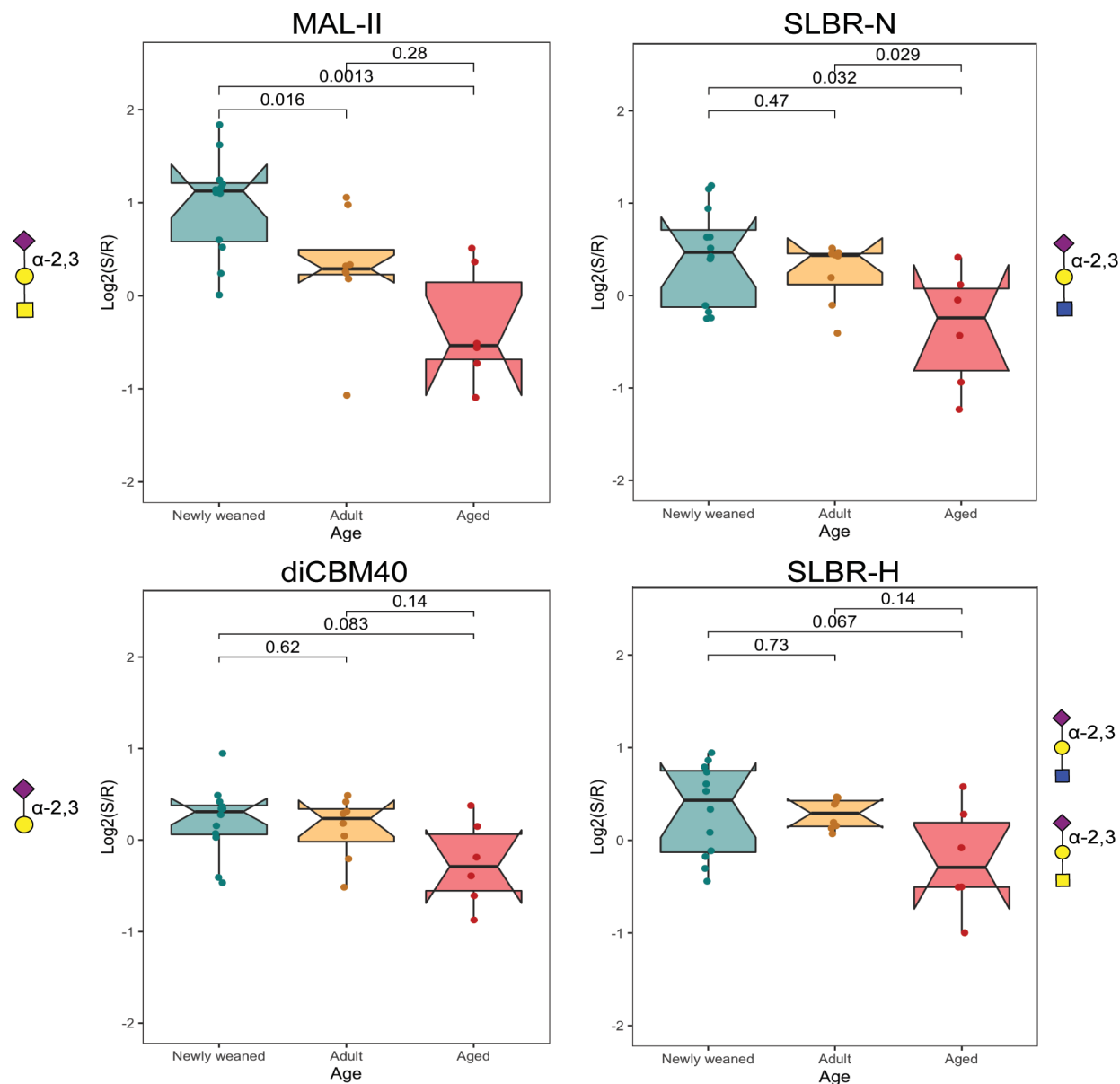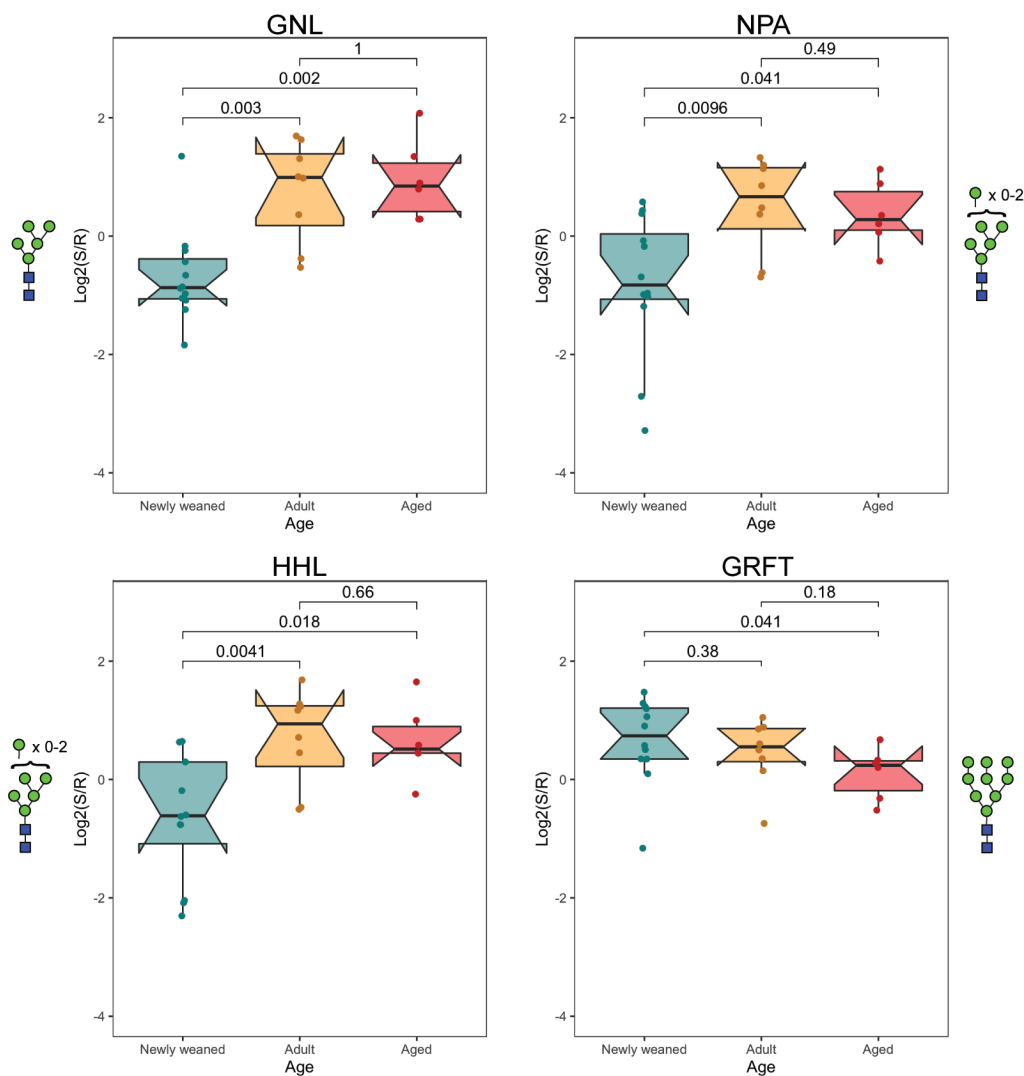
Supplementary Figure S2. Boxplots of α-2,3-sialoside levels by age in uninfected ferrets. Boxplots of binding by $\alpha2,3$-sialic acid lectins (MAL-II, SLBR-N, diCBM40, SLBR-H). Median normalized $\log_2$ ratios (Sample (S)/Reference(R)) are plotted by age (Newly weaned: cyan; Adult: orange; Aged: red). P-value from Wilcoxon's t-test is shown for indicated pairs. Glycans bound by lectins are shown in SNFG at the side of the boxplots.
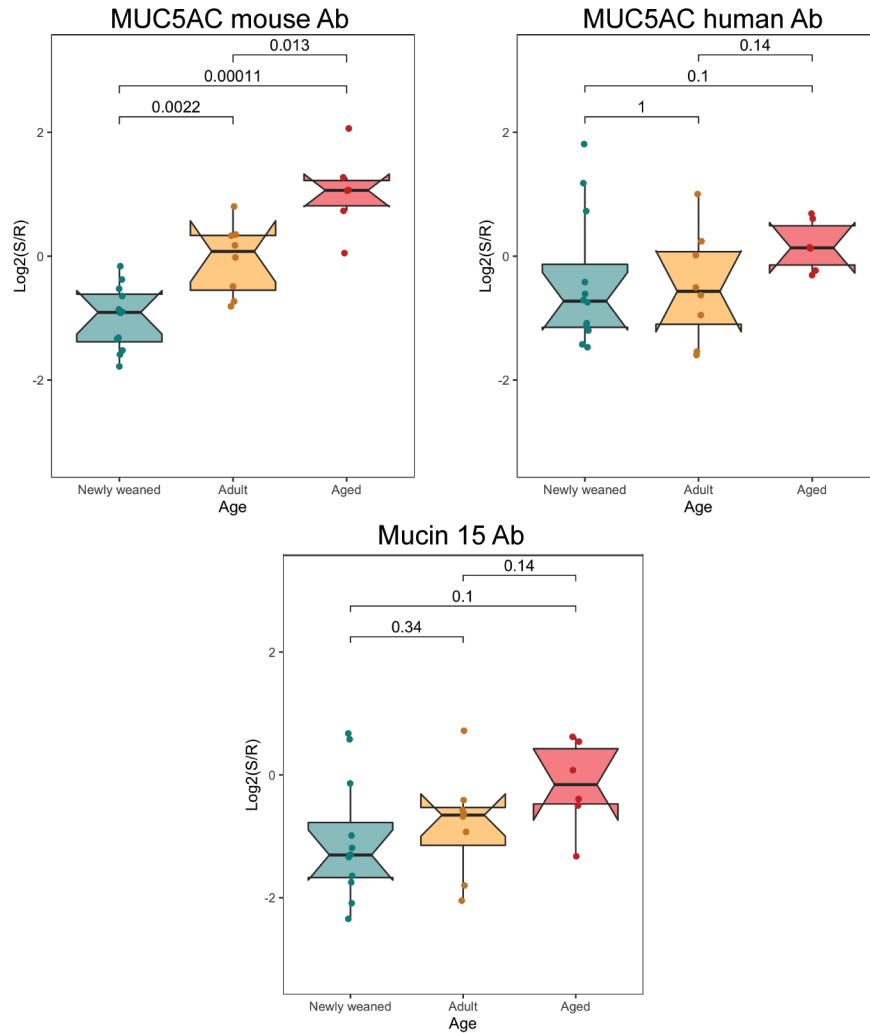
Supplementary Figure S3. Boxplots of mucins expressions by age in uninfected ferrets. Boxplots of binding by mucin antibodies(MUC5AC mouse Ab, MUC5AC human Ab and Mucin 15 Ab). Median normalized $\log_2$ ratios (Sample (S)/Reference(R)) are plotted by age (Newly weaned: cyan; Adult: orange; Aged: red). P-value from Wilcoxon's t-test is shown for indicated pairs.
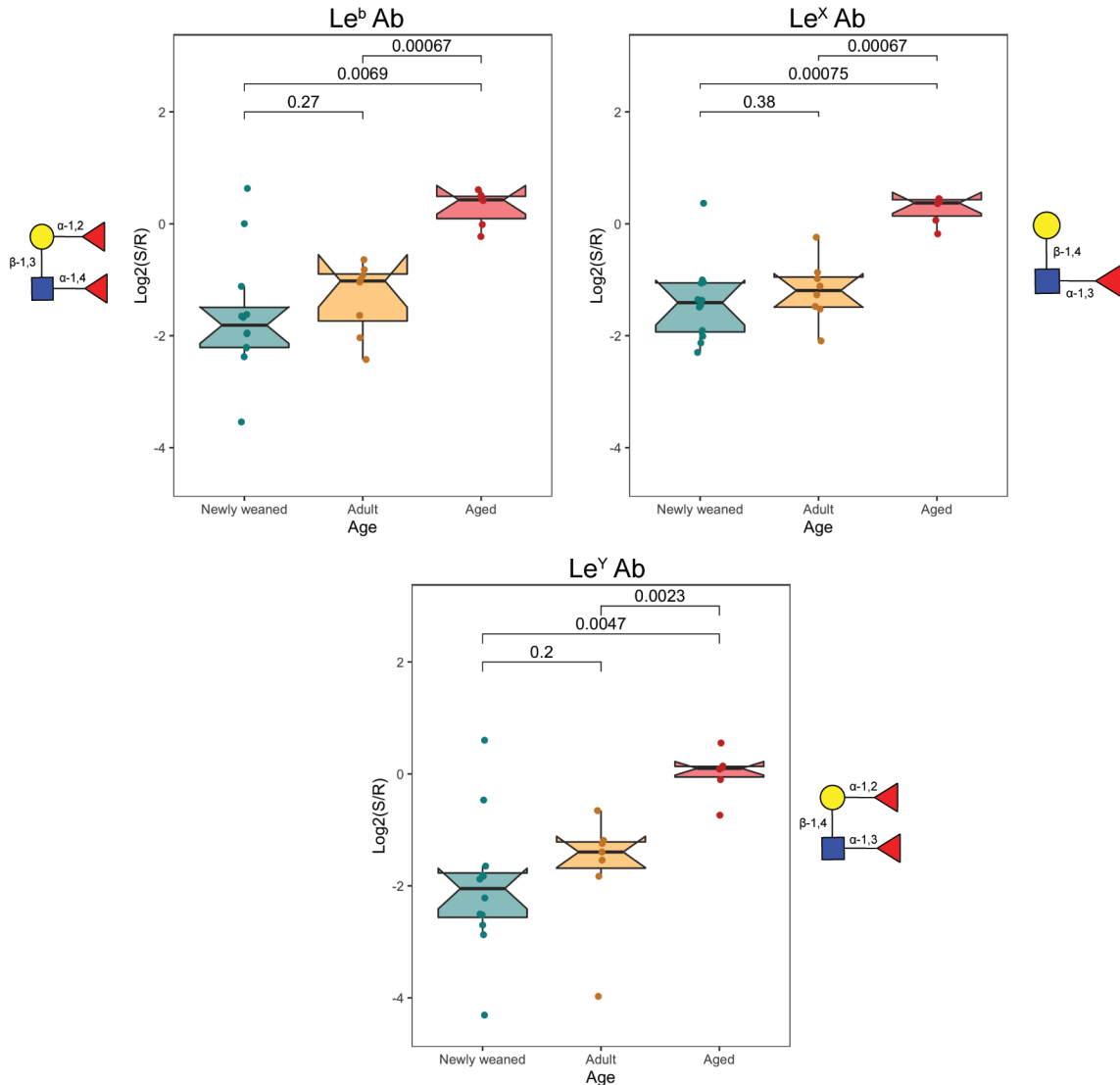
Supplementary Figure S4. Boxplots of Lewis structures by age in uninfected ferrets. Boxplots of binding by Lewis structures antibodies(Le[b] Ab, Le[X] Ab and Le[Y] Ab). Median normalized $\log_2$ ratios (Sample (S)/Reference(R)) are plotted by age (Newly weaned: cyan; Adult: orange; Aged: red). P-value from Wilcoxon's t-test is shown for indicated pairs. Glycans bound by lectins are shown in SNFG at the side of the boxplots.
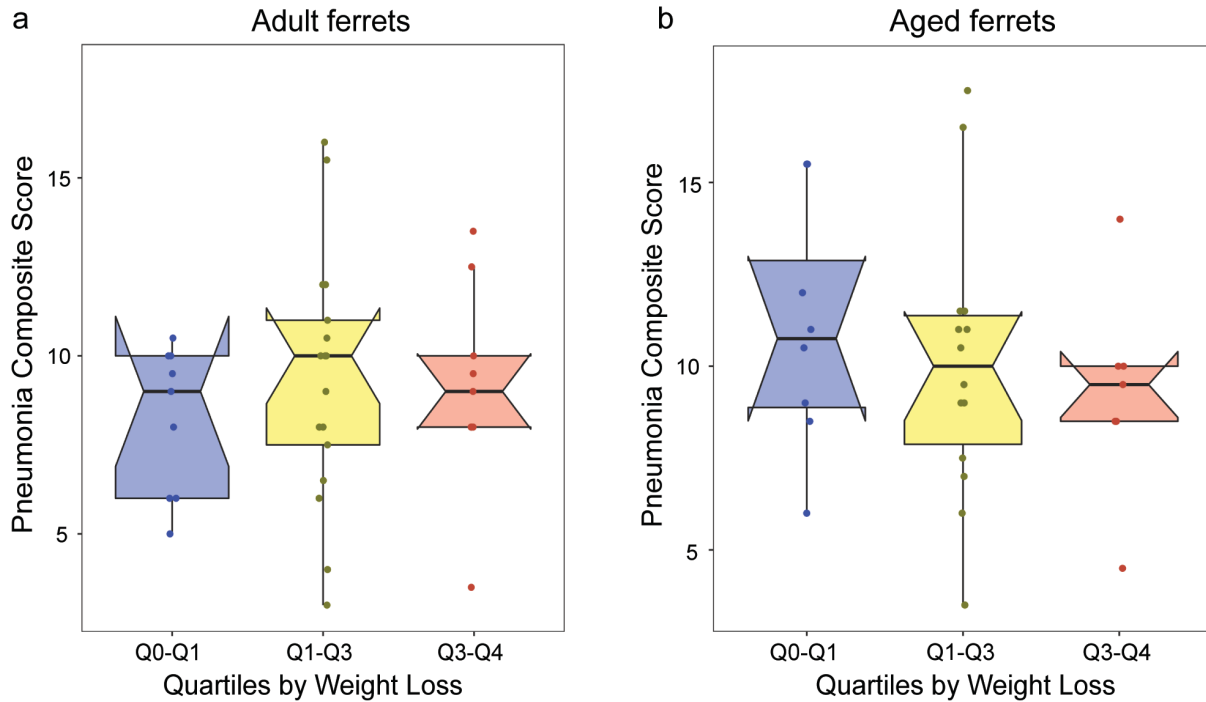
Supplementary Figure S5. Boxplots of high/oligo-mannose levels by age in uninfected ferrets. Boxplots of binding by high/oligo-mannose lectins(GNL, NPA, HHL and GRFT). Median normalized $\log_2$ ratios (Sample (S)/Reference(R)) are plotted by age (Newly weaned: cyan; Adult: orange; Aged: red). P-value from Wilcoxon's t-test is shown for indicated pairs. Glycans bound by lectins are shown in SNFG at the sides of the boxplots.

Supplementary Figure S6. Boxplots of Pneumonia Composite Score (PCS) as a function of weight loss quartiles in adult and aged ferrets. Q0-Q1: 1st quartile (blue), Q1-Q3: middle quartiles (yellow), Q3-Q4: last quartile (red) of weight loss percent. a) Boxplot analysis of PCS correlation to weight loss in adult ferrets at day 8 post-infection with H1N1pdm09. (Q0-Q1, n = 9 ferrets; Q1-Q3, n = 17; Q3-Q4, n = 9). b) Boxplot analysis of correlation in aged ferrets at day 8 post-infection (Q0-Q1, n = 8 ferrets; Q1-Q3, n = 14; Q3-Q4, n = 7).
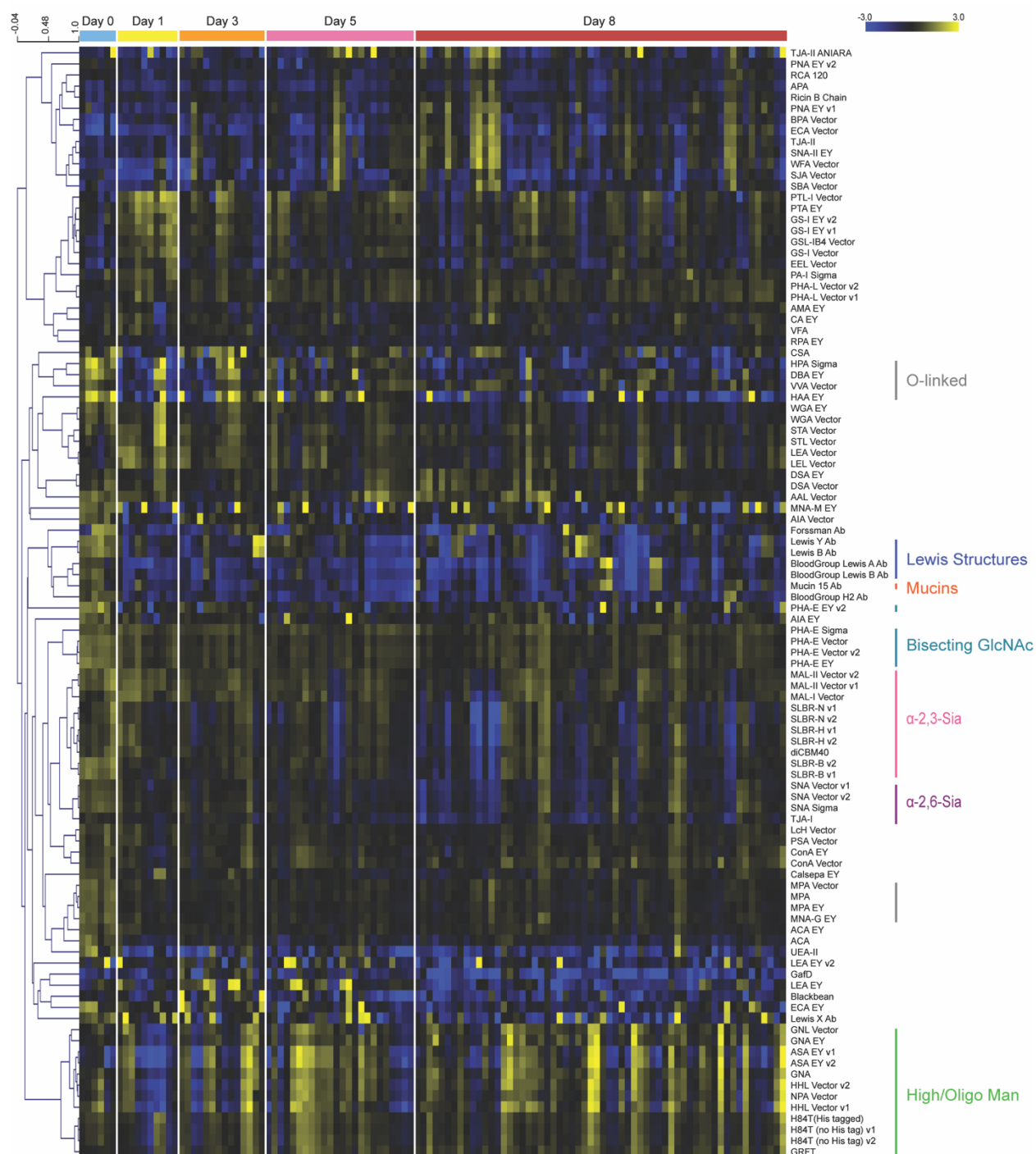
Supplementary Figure S7. Aged ferrets had delayed response to influenza infection. Median normalized $\log_2$ ratios (Sample (S)/Reference(R)) of aged (>5.5 years) ferret lung samples were ordered by days post infection. Uninfected (blue), n = 3; day 1 (yellow), n = 5; day 3 (orange), n = 7; day 5 (pink), n = 12; day 8 (red), n = 29. 2 samples per ferret. Yellow, $\log_2(S) > \log_2(R)$; blue, $\log_2(R) > \log_2(S)$. Lectins binding α-2,3-sialosides (pink), α-2,6-sialosides (purple), high/oligo-mannose (green), bisecting GlcNAc (turquoise), *O*-linked glycans (charcoal), mucins (orange) and Lewis structures (blue) are highlighted on the right of the heatmap.

S9
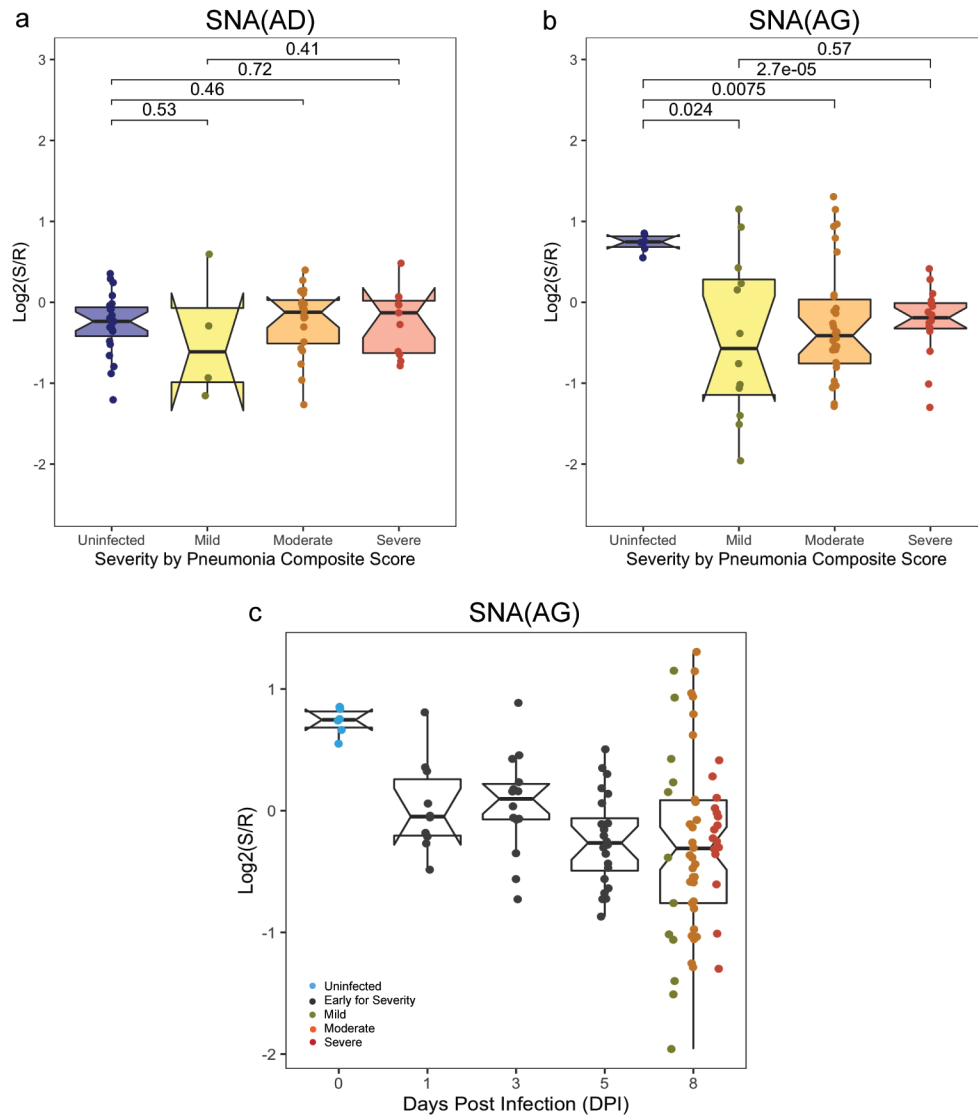
Supplemental Figure S8. Impact of influenza infection on α-2,6-sialosides in adult and aged ferrets. a) Severity study of α-2,6-sialic acids probed by SNA at day 8 post-infection in adult ferrets (AD) is shown. Boxplots of median normalized $\log_2$ ratios (Sample (S)/Reference(R)) of ferret lung samples were ordered by severity defined by pneumonia composite score (PCS). Uninfected (blue): n = 4, 4 samples per ferret. Day 8 post-infection: Mild (yellow), n = 2, 2 samples per ferret; Moderate (orange), n = 11, 2 samples per ferret; Severe (red), n = 6, 2 samples per ferret. b) Severity study of α-2,6-sialic acids probed by SNA at day 8 post-infection in aged ferrets (AG) is shown. Boxplots of median normalized $\log_2$ ratios (Sample (S)/Reference(R)) of ferret lung samples were ordered by severity defined by PCS. Uninfected (blue): n = 3, 2 samples per ferret. Day 8 post-infection (2 samples per ferret): Mild (yellow), n = 6; Moderate (orange), n = 15; Severe (red), n = 8. P-value from Wilcoxon's t-test is shown for indicated pairs. c) Time-course analysis of α-2,6-sialic acid levels probed by SNA following H1N1pdm09 infections (t = 0, 1, 3, 5 and 8 days) in aged animals (AG). Boxplot of median normalized $\log_2$ ratios (Sample (S)/Reference(R)) is shown. Disease severity is indicated by color (Uninfected: blue; Early for Severity: black; Mild: dark yellow; Moderate: orange, Severe: red).

S10
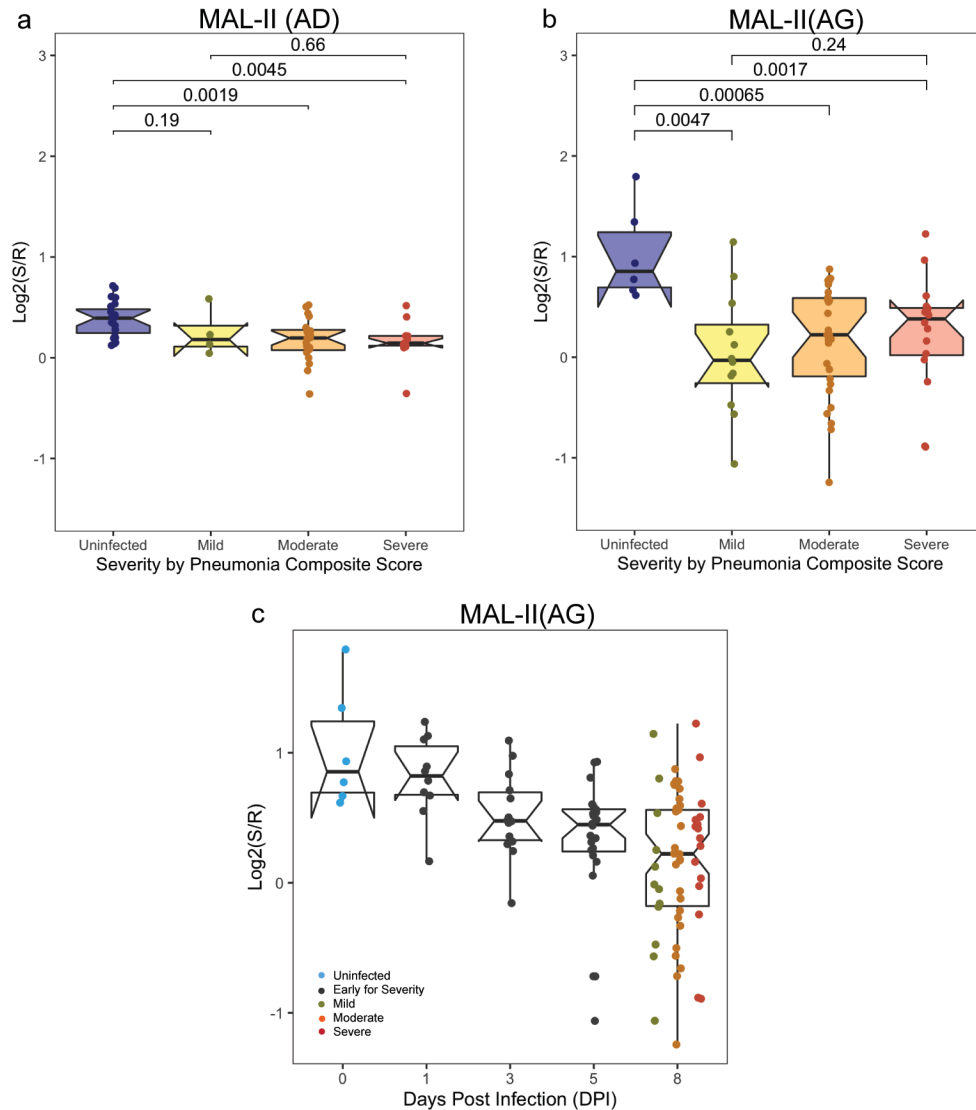
Supplemental Figure S9. Impact of influenza infection on α-2,3-sialosides in adult and aged ferrets. a) Severity study of α-2,3-sialic acids probed by MAL-II at day 8 post-infection in adult ferrets (AD) is shown. Boxplots of median normalized $\log_2$ ratios (Sample (S)/Reference(R)) of ferret lung samples were ordered by severity defined by pneumonia composite score (PCS). Uninfected (blue): n = 4, 4 samples per ferret. Day 8 post-infection: Mild (yellow), n = 2, 2 samples per ferret; Moderate (orange), n = 11, 2 samples per ferret; Severe (red), n = 6, 2 samples per ferret. b) Severity study of α-2,3-sialic acids probed by MAL-II at day 8 post-infection in aged ferrets (AG) is shown. Boxplots of median normalized $\log_2$ ratios (Sample (S)/Reference(R)) of ferret lung samples were ordered by severity defined by PCS. Uninfected (blue): n = 3, 2 samples per ferret. Day 8 post-infection: Mild (yellow), n = 6, 2 samples per ferret; Moderate (orange), n = 15, 2 samples per ferret; Severe (red), n = 8, 2 samples per ferret. P-value from Wilcoxon's t-test is shown for indicated pairs. c) Time-course analysis of α-2,3-sialic acid levels probed by MAL-II following H1N1pdm09 infections (t = 0, 1, 3, 5 and 8 days) in aged animals (AG). Boxplot of median normalized $\log_2$ ratios (Sample (S)/Reference(R)) is shown. Disease severity is indicated by color (Uninfected: blue; Early for Severity: black; Mild: dark yellow; Moderate: orange, Severe: red).
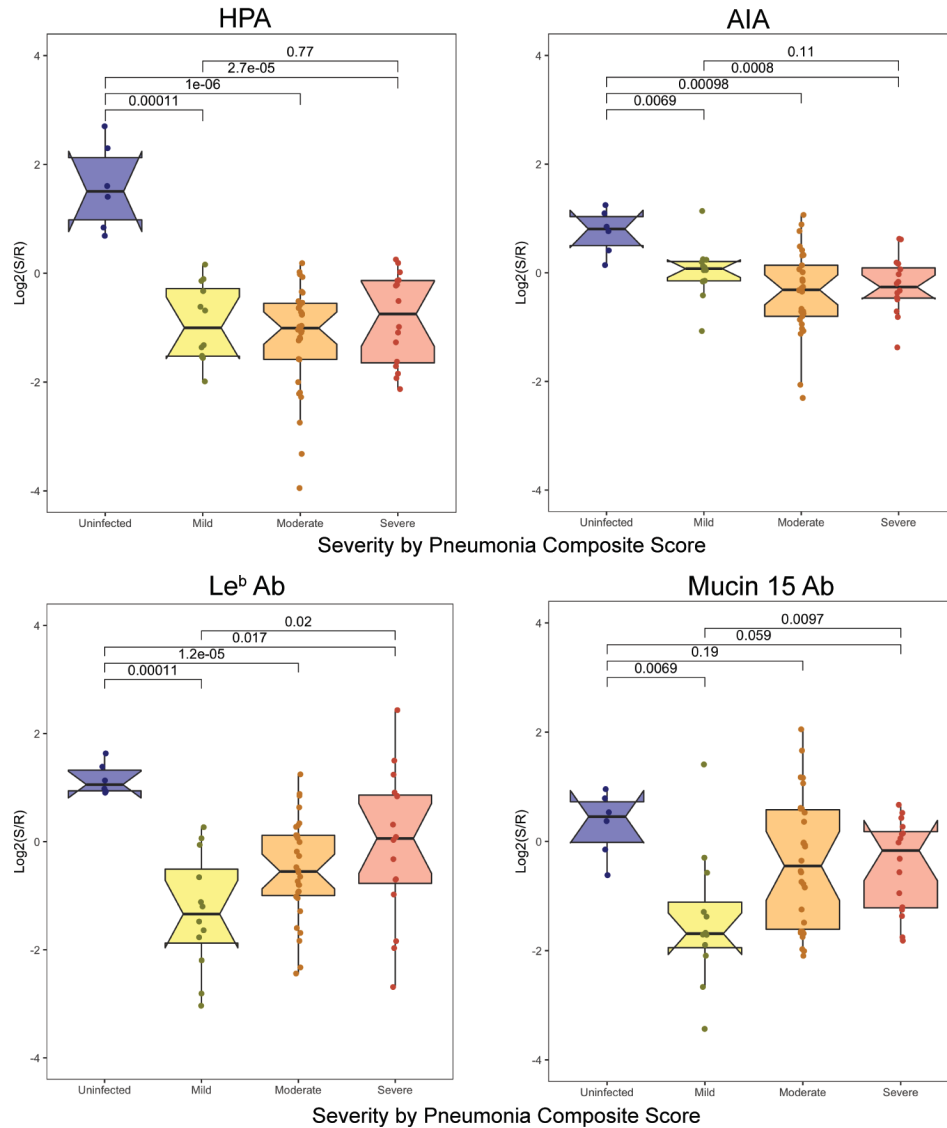
Supplemental Figure S10. Impact of influenza infection on *O*-linked glycans in aged ferrets. Severity study of *O*-linked glycans probed by HPA and AIA, Lewis structures by Le^b Ab, and mucins by Mucin 15 Ab at day 8 post-infection in aged ferrets is shown. Boxplots of median normalized log_2 ratios (Sample (S)/Reference(R)) of ferret lung samples were ordered by severity defined by PCS. Uninfected (blue): n = 3, 2 samples per ferret. Day 8 infected: Mild (yellow), n = 6, 2 samples per ferret; Moderate (orange), n = 15, 2 samples per ferret; Severe (red), n = 8, 2 samples per ferret. P-value from Wilcoxon's t-test is shown for indicated pairs.
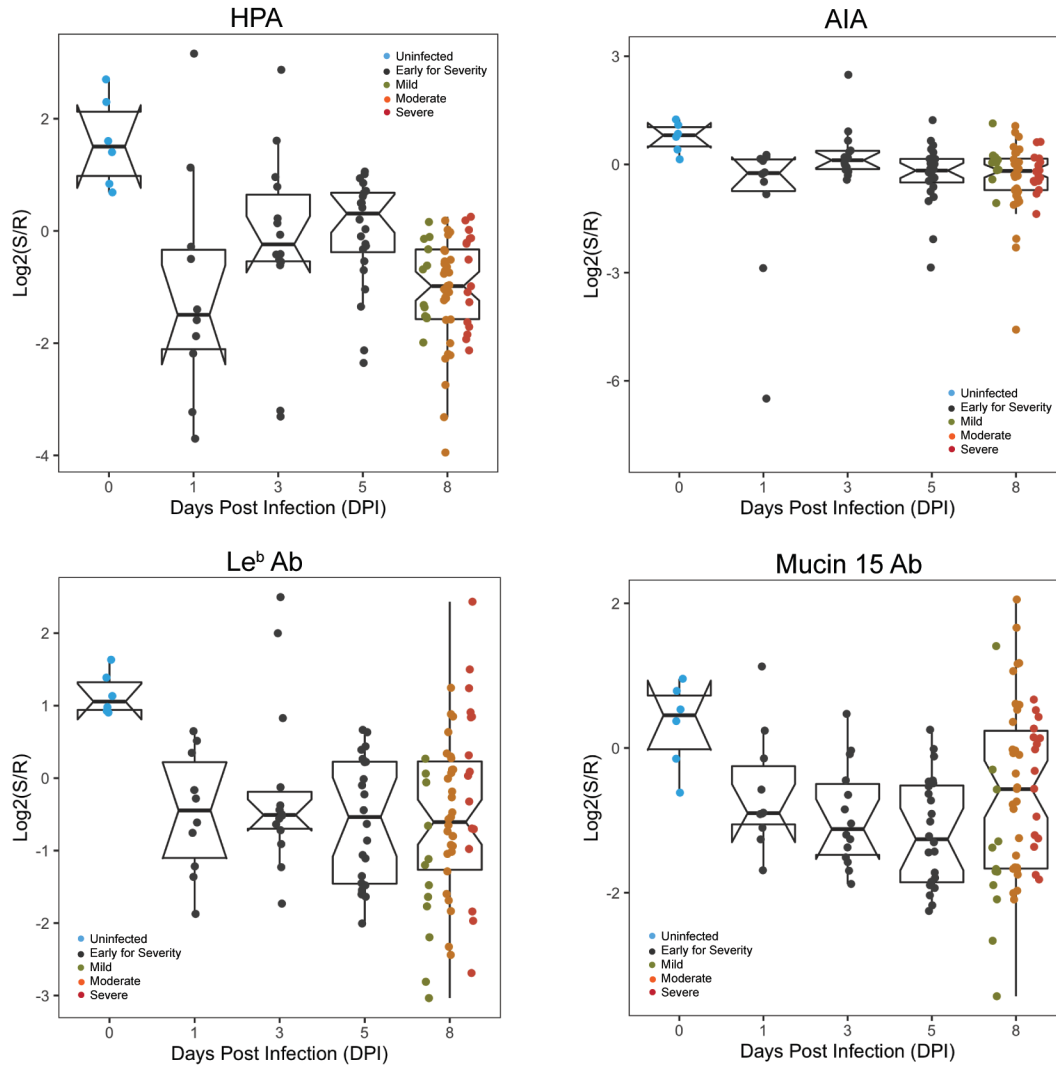
Supplementary Figure S11. Dynamic changes in *O*-linked glycans are observed upon infection in aged ferrets. Boxplot analysis of *O*-linked glycans probed by HPA and AIA, Lewis structures probed by Le^b Ab, and mucins probed by Mucin 15 Ab following H1N1pdm09 infections (t = 0, 1, 3, 5 and 8 days). Boxplot of median normalized log$_2$ ratios (Sample (S)/Reference(R)) is shown. Disease severity is indicated by color (Uninfected: blue; Early for Severity: black; Mild: dark yellow; Moderate: orange, Severe: red).
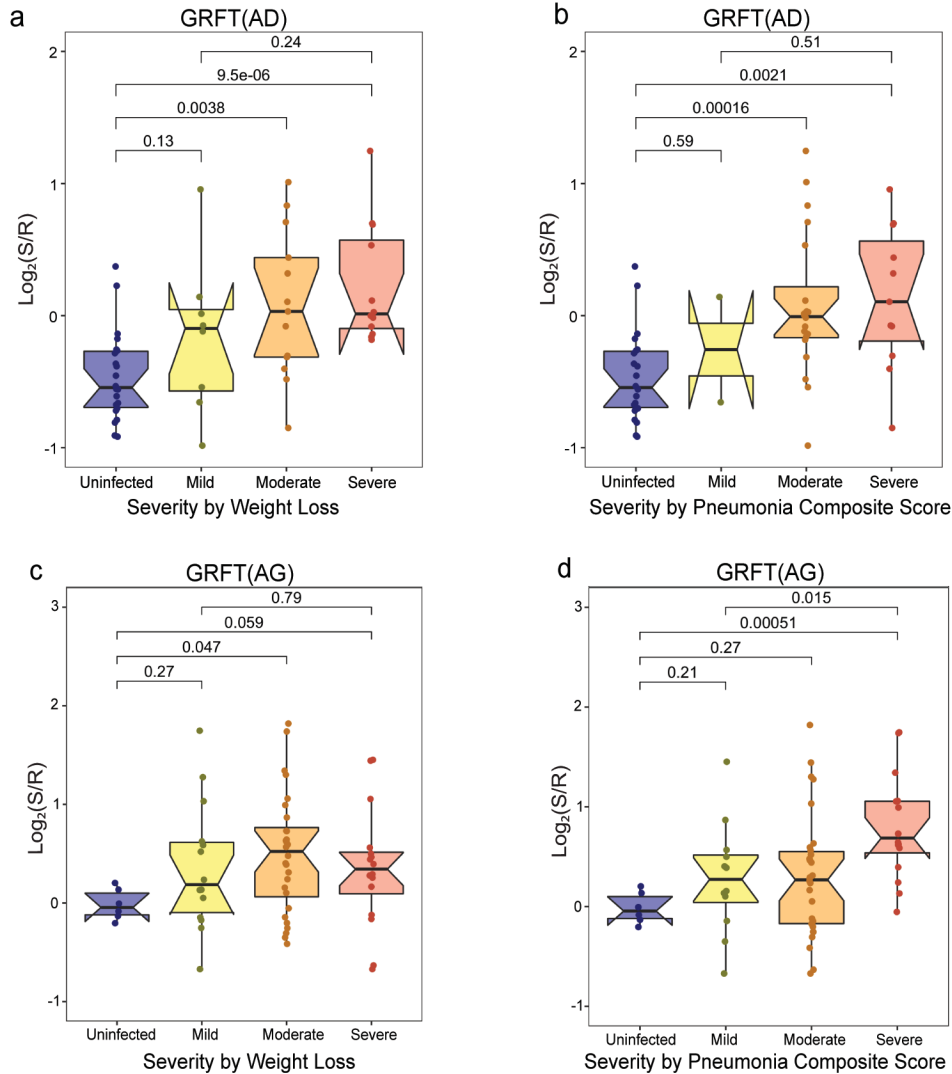
Supplementary Figure S12. Comparison of severity metrics used in adult and aged ferrets.
a) Boxplot analysis of lectin binding by GRFT (high-mannose) as a function of severity defined by weight loss in adult ferrets (AD). Uninfected (blue): n = 4, 4 samples per ferret. Day 8 post-infection: Mild (yellow), n = 5, 2 samples per ferret; Moderate (orange), n = 7, 2 samples per ferret; Severe (red), n = 7, 2 samples per ferret. b) Boxplot analysis of lectin binding by GRFT (high-mannose) as a function of severity defined by pneumonia composite score (PCS) in adult ferrets (AD). Uninfected (blue): n = 4, 4 samples per ferret. Day 8 post-infection: Mild (yellow), n = 2, 2 samples per ferret; Moderate (orange), n = 11, 2 samples per ferret; Severe (red), n = 6, 2 samples per ferret. c) Boxplot analysis of lectin binding by GRFT (high-mannose) as a function of severity defined by weight loss in aged ferrets (AG). Uninfected (blue): n = 3, 2 samples per ferret. Day 8 post-infection: Mild (yellow), n = 7, samples per ferret; Moderate (orange), n = 14, 2 samples per ferret; Severe (red), n = 8, 2 samples per ferret. d) Boxplot analysis of lectin binding by GRFT (high-mannose) as a function of severity defined by PCS in aged ferrets (AG). Uninfected (blue): n = 3, 2 samples per ferret. Day 8 post-infection: Mild (yellow), n = 6, 2 samples per ferret; Moderate (orange), n = 15, 2 samples per ferret; Severe (red), n = 8, 2 samples per ferret.
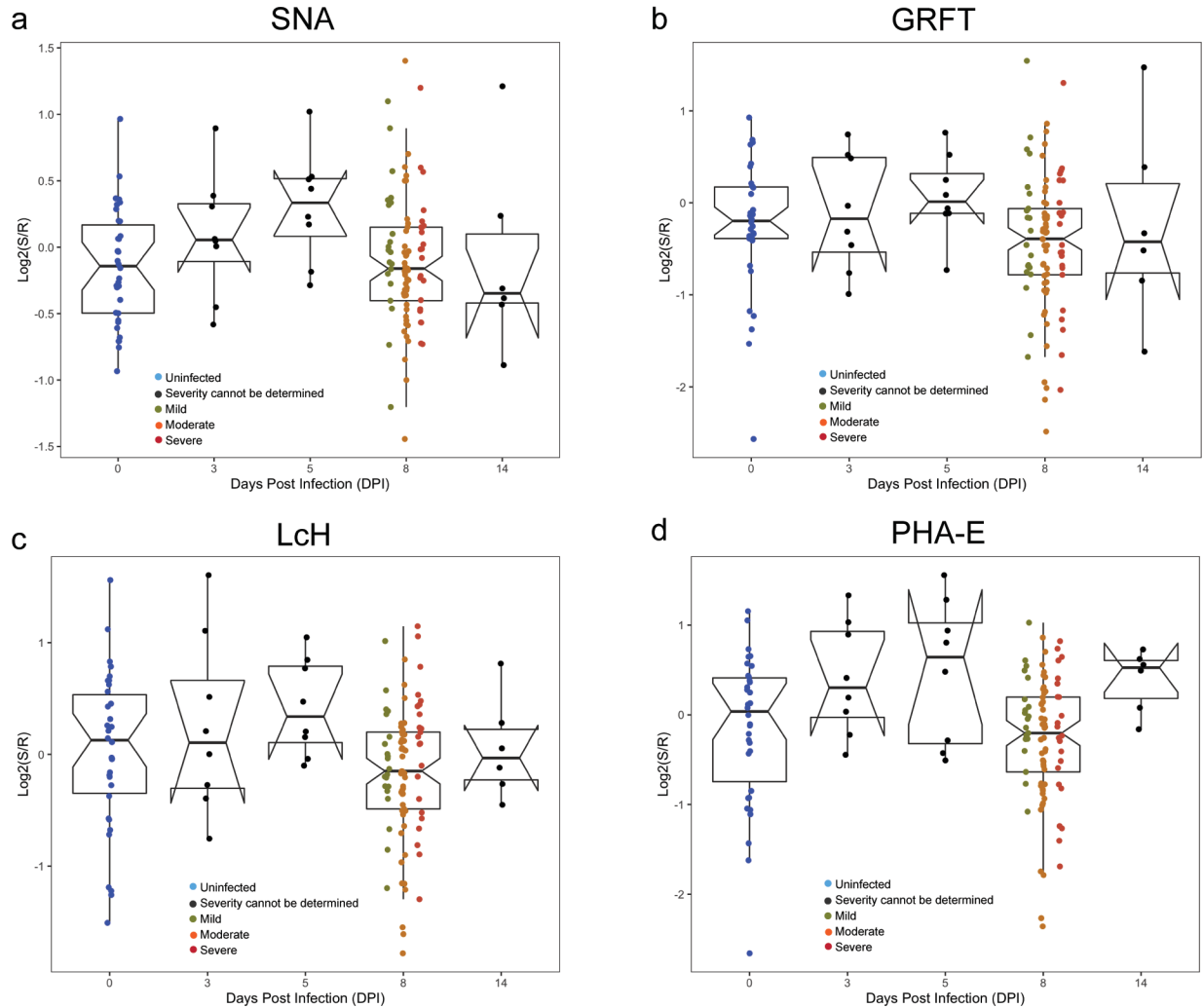
Supplementary Figure S13. Glycan changes are observed early in the time-course study of newly weaned ferrets. a) Time-course analysis of α-2,6-sialic acid probed by SNA following H1N1pdm09 infections (t = 0, 3, 5, 8 and 14 days). b) Time-course analysis of high/oligo-mannose probed by GRFT. c) Time-course analysis of core fucose probed by LcH. d) Time-course analysis of bisecting branching probed by PHA-E. Boxplot of median normalized $\log_2$ ratios (Sample (S)/Reference(R)) is shown. Disease severity is indicated by color (Uninfected: blue; Severity cannot be determined: black; Mild: dark yellow; Moderate: orange, Severe: red).

Supplemental Table 1. Lectins used in microarrays

Lectin	Species/Origin	Print Conc. (μg/mL)	Rough Specificity /Inhibitory monosaccharide	Vendor/Source
AAL [a,b,c]	*Aleuria aurantia*	1000	Fucose	Vector
ACA [a,b,c]	*Amaranthus Caudatus*	1000	Gal-β1,3-GalNAc	Vector
AIA [a,b,c]	*Artocarpus integrifolia*	500	β1,3-GalNAc	Vector/EY
AMA [a,b,c]	*Allium moly*	500	Oligo mannose	EY
Anti-B.G.B [CLCP-19B] [a]	MAb mouse IgM [CLCP-19B]	undiluted	Blood group B antigen	Abcam
Anti-B.G.H2 [a,b,c]	MAb mouse IgM [A46-B/B10]	undiluted	Blood group H2 antigen	Santa Cruz Biotechnology
Anti-CD 15[MY-1] [a]	Mab mouse IgM [MY-1]	undiluted	Lewis X	Abcam
Anti-B.G. Lewis A [7LE] [b,c]	MAb mouse IgG1 [7LE]	undiluted	Lewis A	Abcam
Anti-B.G. Lewis B [2-25LE] [b,c]	MAb mouse IgM [2-25LE]	undiluted	Lewis B	Abcam
Anti-B.G.Lewis Y [b,c]	MAb mouse IgM	undiluted	Lewis Y	Santa Cruz Biotechnology
Anti-Forssman [117C9] [a,b,c]	MAb Rat IgM [117C9]	undiluted	Forssman Antigen	Abcam
Anti-Lewis B [T218] [a,b,c]	IgM [T218]	undiluted	Lewis B	Sigma
Anti-Lewis X [P12] [a,b,c]	MAb mouse IgM [P12]	undiluted	Lewis X	Abcam
Anti-Lewis Y [F3] [a,b,c]	MAb mouse IgM [F3]	undiluted	Lewis Y	Abcam
Anti-MUC5AC human [CLH2] [b]	Mab mouse IgG1 [CLH2]	undiluted	human MUC5AC	Sigma
Anti-MUC5AC mouse [b]	Goat polyclonal to mouse MUC5AC	undiluted	mouse MUC5AC	LSBio
Anti-Mucin 15 [H-5] [b,c]	Mab mouse IgG1 [H-5]	undiluted	Mucin 15	Santa Cruz Biotechnology
AOL [a,b,c]	*Aspergillus oryzae*	1000	Fucose	TCI America
APA [a,b,c]	*Abrus precatorius*	500	Gal-β1,3-GalNAc / Lac	EY
APP [a]	*Aegopodium podagraria*	1000	GalNAc / Lac / Gal	EY
ASA [a,b,c]	*Allium sativum*	1000	Mannose	EY
BDA [a]	*Bryonia dioica*	1000	GalNAc / Lac	EY

Blackbean [a,b,c]	*Blackbean crude*	1000	GalNAc	EY
BPA [a,b,c]	*Bauhinia purpurea*	500	β-Gal / β-GalNAc	Vector
CA [a,b,c]	*Colchicum autumnale*	1200	Bi-antennary N-linked glycans	EY
CAA [a]	*Caragana arborescens*	1000	Bi-antennary N-linked glycans	EY
Calsepa [b,c]	*Calystegia sepium*	1000	Bisecting N-linked glycans	EY
CCA [a]	*Cancer antennarius*	1000	9-O-Acetly sialylation / 4-O-Acetyl sialylation	EY
Cholera Toxin [b]	*Vibrio cholerae*	1000	GM1 ganglioside	Sigma
Con A [b,c]	*Canavalia ensiformis*	1000	Tri-mannose core	EY/Vector
CSA [a,b,c]	*Cystisus scoparius*	1000	Terminal GalNAc	EY
DBA [a,b,c]	*Dolichos Biflorus*	1000	GalNAc	Vector
diCBM40 [a,b,c]	engineered NanI from *Clostridium perfringens*	1000	α Sialylation	Generated in house
DSA [a,b,c]	*Datura stramonium*	500	LacNAc	EY/Vector
ECA [a,b,c]	*Erythrina cristagalli*	1000	LacNAc	Vector
EEL/EEA [a,b,c]	*Eunonymus europaeus*	1000	Blood Group B	Vector/EY
GafD [a,b,c]	recombinant GafD from *Escherichia coli*	1000	GlcNAc	Generated in house
GNA/GNL [a,b c]	*Galanthus nivalis*	1500	Oligo mannose	Vector/EY
GHA [a]	*Glechoma hederacea*	500	GalNac	EY
GS-I [a,b,c]	*Griffonia simplicifoia-I*	1000	α-Gal / Lac	Vector/EY
GS-II [a,b,c]	*Griffonia simplicifoia-II*	1000	GlcNAc	Vector
GS-IB4 [a,b,c]	*Griffonia simplicifoia-I, isolectin B4*	2000	Gal	Vector
H84T [b,c]	*Banana lectin*	1000	High mannose	Gift from Dr. David Markovitz
HAA [a,b,c]	*Homarus americanus*	1000	Terminal GalNAc	EY

HHL [a,b,c]	*Hippeastrum Hybrid*	1500	Oligo/High mannose	Vector
HPA [a,b,c]	*Helix pomatia*	1000	Blood Group A	Sigma/EY
IRA [a]	*Iris Hybrid*	1000	GalNAc / Lac	EY
LBA [a]	*Phaseolus lunatus*	1000	Blood Group A	EY
LAA [b]	*Laburnum alpinum*	900	GlcNAc	EY
LcH [a,b,c]	*Lens Culinaris*	1000	Core Fucose	Vector
LEA/LEL [a,b,c]	*Lycopersicon esculentum*	1000	GlcNAc	Vector/EY
LFA [a]	*Limax flavus*	500	α Sialylation	EY
Lotus [a,b,c]	*Lotus tetragonolobus*	1000	Fucose	Vector
MAA [a]	*Maackia amurensis*	500	Sialylation/Sulfation	EY
MAL-I [a,b,c]	*Maackia amurensis-I*	2000	Sialylation/Sulfation	Vector
MAL-II [a,b,c]	*Maackia amurensis-II*	2000	Sialylation/Sulfation	Vector
MNA-G [a,b,c]	*Morus nigra Morniga G*	1000	GalNAc	EY
MNA-M [a,b,c]	*Morus nigra Morniga M*	1000	Oligo mannose / Gal	EY
MPA/MPL [a,b,c]	*Maclura pomifera*	1000	β1,3-GalNAc	Vector
newBR6 [b]	unknown (from unpublished work)	480	under investigation	Gift from Dr. Barbara Bensing
NPA [a,b,c]	*Narcissus pseudonarcissus*	1000	Oligo mannose	Vector
PA-I [a,b,c]	*Pseudomonas aeruginosa*	1000	Gal	Sigma
PA-IL [a]	*bacteria*	1000	GalNAc	Generated in house
PHA-E [a,b,c]	*Phaseolus vulgaris Erythroagglutinin*	1000	Bisecting GlcNAc	Vector/EY/Sigma
PHA-L [a,b,c]	*Phaseolus vulgaris Leukoagglutinin*	1000	β1,6 Branching N-Link glycans	Vector/EY
PMA [a]	*Polygonatum multiflorum*	500	Oligo mannose	EY
PNA [a,b,c]	*Arachis hyogaea*	1000	Gal-β1,3-GalNAc	Vector/EY
PSA [a,b,c]	*Pisum sativum*	1000	Core Fucose	Vector
PSL [a]	*Polyporus squamosus*	1000	α2,6 sialylation	EY
PTA [a,b,c]	*Psophocarpus tetragonolobus*	500	Blood Groups	EY

PTL-I [a,b,c]	*Psophocarpus tetragonolobus-I*	1500	Blood Group A	Vector
PTL-II [a,b,c]	*Psophocarpus tetragonolobus-II*	1000	α2 Fucose	Vector
RCA120 [a,b,c]	*Ricinus Communis Agglutinin I*	1000	Gal / Lac	Vector
rCVN [a]	*recombinant Cyanovirin*	1000	High mannose	Gift from Dr. Barry O'Keefe
rGRFT [a,b,c]	*recombinant Griffithsin*	1000	High mannose	Gift from Dr. Barry O'Keefe
Ricin B Chain [a,b,c]	*Ricinus communis*	1000	Gal	Vector
RPA [a,b,c]	*Robinia pseudoacacia*	500	Complex N-link glycans	EY
rSVN [a,b]	*recombinant Scytovirin*	1000	High mannose	Gift from Dr. Barry O'Keefe
SBA [a,b,c]	*Glycine max*	1000	LacdiNAc	Vector
SJA [a,b,c]	*Sophora japonica*	1000	LacdiNAc	Vector
SK1 [b]	*Streptococcus sanguinis SK1*	1800	α2,3 sialylation	Gift from Dr. Barbara Bensing
SK678 [b]	*Streptococcus sanguinis SK678*	450	α2,3 sialylation	Gift from Dr. Barbara Bensing
SLBR-B [b,c]	*Streptococcus gordonii M99*	1000	α2,3 sialylation	Gift from Dr. Barbara Bensing
SLBR-H [b,c]	*Streptococcus gordonii DL1*	2000	α2,3 sialylation	Gift from Dr. Barbara Bensing
SLBR-N [b,c]	*Streptococcus gordonii UB10712*	1000	α2,3 sialylation	Gift from Dr. Barbara Bensing
SNA [a,b,c]	*Sambucus nigra*	500/1000	α2,6 sialylation	Vector/Sigma
SNA-II [a,b,c]	*Sambucus nigra-II*	1000	α2 Fucose /oligo mannose	EY
STA/STL [a,b,c]	*Solanus tuberosum*	500	GlcNAc	Vector
TJA-I [a,b,c]	*Trichosanthes japonica-I*	1000	α2,6 sialylation	TCI
TJA-II [a,b,c]	*Trichosanthes japonica-II*	1000	α2 Fucose	NorthStar Bioproducts/Aniara Diagnostica
TL [a,b,c]	*Tulipa sp.*	700	GlcNAc	EY
UDA [a,b]	*Urtica dioica*	1000	GlcNAc / Oligo mannose	EY
UEA-I [a,b,c]	*Ulex europaaeus-I*	1000	α2 Fucose	Vector
UEA-II [a,b,c]	*Ulex europaaeus-II*	2000	GlcNAc	Vector
VFA [a,b,c]	*Vicia faba*	1000	GlcNAc	EY

VVA [a,b,c]	*Vicia villosa*	1000	Terminal GalNAc	Vector/EY
VVA(man) [a,b,c]	*Vicia villosa*	500	Mannose	Vector/EY
WFA [a,b,c]	*Wisteria floribunda*	1000	GalNAc-β1,4	Vector
WGA [a,b,c]	*Triticum vulgare*	1000	GlcNAc	Vector/EY
X408 [b]	unknown (from unpublished work)	1200	under investigation	Gift from Dr. Barbara Bensing

[a] : lectins printed in uninfected experiment
[b] : lectins printed in newly weaned experiment
[c] : lectins printed in aged experiment